UNIVERSIDAD POLITÉCNICA DE CARTAGENA

Proyecto Final de Carrera

DISEÑO DE APLICADORES BASADO EN ANTENAS "LEAKY-WAVE" PARA LA CONFORMACIÓN DE PATRONES DE CAMPO ELÉCTRICO CERCANO

Applicator Design based in Leaky-wave Antennas for the Near Electric-Field Beam Pattern Shiping

Autor: Adriana Pérez García
Director: D. José Luis Gómez Tornero
Codirector: D. Juan Monzó Cabrera

20 de septiempre de 2016

Dedicado a
mi madre y a mi hermana

Agradecimientos

Quisiera dar las gracias lo primero de todo a mis tutores y directores de proyecto, *Juan Monzó* y *José Luis Gómez Tornero*, por motivarme y haber hecho que me interese en lo que me gusta, ofreciéndome oportunidades inolvidables, haciendo que haya aprendido a valerme por mí misma en el mundo laboral, y también por los conocimientos que tan generosamente me han transmitido.

Estudiar ingeniería ha sido una carrera de fondo, y sin las personas que me llevo de aquí, mis amigos incondicionales, mi experiencia hubiera sido distinta y mucho más dura. Por eso gracias a *Alejandro, Antonio, David y Jackson* por ser esos compañeros envidiables y que han estado de principio a fin pasando todos esos exámenes, trabajos y prácticas, pero sobretodo esos momentos especiales fuera de las aulas.

Sin embargo, hay un compañero, que lejos de ser sólo el mejor amigo que he tenido y tendré, se convirtió en algo extraordinario. Desde el primer día en el autobús para ir a la primera clase en el Aula 1.1 de Antiguones, hasta hoy, y que por siempre ocupará un lugar privilegiado, el que ha sido, es y será mi mitad fundamental en esta etapa universitaria pero sobretodo en mi vida. A *Víctor Chacón López*, la mejor persona que he conocido nunca, que me has dado color a lo negro y luz a la oscuridad, gracias por creer en mí, por valorarme y confiar en mí de esa manera. Nos quedan muchísimas cosas por compartir y vivir y no puedo estar más alegre y orgullosa de que sé que lo podemos hacer y lo haremos juntos.

Dar las gracias también a *mi Abuela*, que con su sabiduría y experiencia, ha sido mi segunda madre, y el pilar para que todo cuadre como un puzzle y me hace sentir una de las personas más especiales en el mundo, pero también a *mi Abuelo*, que aunque falte, me transmite su calor y su orgullo.

Nunca podré tomar mejor referencia ni mayor ejemplo que con la persona a la que más admiro, quiero y respecto sobre todas las cosas, la más fuerte, luchadora y que más se ha desvivido por lograr que lleguemos siempre a lo más alto, *mi Madre*, que ha hecho posible mis sueños y me ha otorgado el orgullo de ser su hija, y que sin ella sé que estaría totalmente perdida . Pero no puedo olvidar a la tercera parte de esta trinidad, *mi Hermana pequeña*, que a veces me demuestra que podría ser la mayor, que como psicóloga que es, sabe siempre qué decir y cómo hacerlo para que todo se torne maravilloso, no sólo es mi hermana, sino mi mayor apoyo y mi mejor amiga en el mundo y que todos los días es capaz de enseñarme algo nuevo. Sin ellas, todo esto sería en vano.

Y por supuesto, a esa persona ausente pero que siempre está presente, a *mi Padre*, que sé que me ha acompañado siempre desde arriba y que me ha dado la fuerza cada día para continuar y no desfallecer, siempre he sabido que no andaba sóla y es porque tengo un ángel que me cuida. Gracias.

Contents

List of Figures

List of Tables

Chapter 1

Introduction

Uniform heating on the entire sample volume, or definition of prescribed heating patterns to increase the heating efficiency on determined zones of the sample, is a generally desired capability of modern microwave heating systems. However, the synthesis of heating patterns is still a challenging objective in microwave heating applications.

In this project [1], a phased array of antennas has been proposed with this objective on mind [2–4]: by properly exciting each individual radiator amplitude and phase, near-field focused patterns can be synthesized. Phased-array antennas need for complicated feeding network which distribute the input signal to each radiator with the appropriate amplitude and phase.

Another type of antennas which can synthesize near-field focused patterns, while avoiding complicated feeding networks are Leaky-wave antennas (LWAs). To this aim, the antenna can be curved along its length [5] [6], or the antenna dimensions can be modulated [7], so that the radiated electromagnetic energy is focused in the prescribed zone where the sample is to be heated. On the other hand, the LWA can be curved and modulated at the same tame to optimize the focusing pattern as proposed in [8] [9]. Also, it must be mentioned that LWAs provide a simple mechanism to dynamically shape the focusing pattern by using multi-tone signals as described in [10]. For all these reasons, LWAs are a promising radiator technology to consider in future microwave heating ovens where specific heating patterns need to be obtained.

However, all previous studies with near-field focused LWAs have treated the synthesis of a near-field focused zone in free space, but no attempt has been done yet to synthesize different heating patterns considering the sample to be heated and the microwave oven. In this work, a preliminary study using a phased array of antennas is developed to consider in the future the use of cylindrically curved LWAs which radiate inside a cylindrical metallic oven, with the general aim to demonstrate its capability to shape the heating pattern inside a given sample at a frequency of 2.45GHz, used in microwave applications.

The motivation of this project is the wide variety of possibles applications involved in this research. For instance, those with biomedical purposes as hyperthermia therapy in cancer treatment. Hence, it would be interesting being aware of this concept related to the creation of heating patterns to finally develop advanced techniques which helps society.

1.1 Objectives

The main objective of this project is to obtain a good result that demonstrates the creation of different heating patterns by properly creating a structure capable of heating a dielectric sample of high losses while avoiding overheating on edges or an uneven heating distribution in its whole volume.

Also, this project suposes a starting point to keep investigating about shaping and provides a path to develop other improved techniques and synthesis to take incto acccount in the future of not only microwave applications, but also radiating antennas.

1.2 Report Structure

This report has been subdivided in a total of 5 chapters.

In this *first chapter* an initial approach of the contents of the report is covered, as well as the main objectives of this study and the design approach to be followed.

The *second chapter* will lead us to take a look at the fundamentals of concepts treated as hyperthermia, leaky-wave antennas and array of antennas in order to understand better the motivation and objectives of this work.

In the *third chapter* we will start dealing with the structure design implementation, showing the dimension of the cavities and antennas whose measurments have been properly chosen and optimized to provide the best adaptation result at the resonancy frequency.

In the *fourth chapter* we will begin the results section which have been represented with the results exported from CST to Matlab. Moreover, it illustrates the unsimilar heating distribution collected depending on which antenna or combination of antennas are exciting the oven.

Then, we will move to the *fifth and last chapter* of the report where we will interpret the findings solved in the previous chapter thus, several conclusions will be drawn. Also, the design techniques needed in the future to achieve our objectives and to enhace research, will take part in this final chapter.

1.3 Software Tools Involved

This project is mostly optimization-based, thereby there are not many software implementations. Instead, commercial software such as CST Microwave Studio Suite has been used [11]. Besides, some Matlab scripts have been developed to allow the file conversion and represent the final results.

CST offers products suitable for a wide range of electromagnetic design tasks, capable of simulating numerous components and systems.

Together, the products in the CST STUDIO SUITE family can carry out electrostatic and magnetostatic, stationary, low-frequency and high-frequency simulations, as well as being able to calculate the effects of EM fields on substances as diverse as magnetic materials, biological tissues and charged particles. Tight integration with third party tools extends the application range even further.

Passive microwave & RF component design is a major application of CST STUDIO SUITE, and supporting it is one of CST's core competencies. Design engineers use the exceptional performance of CST MICROWAVE STUDIO (CST MWS) for developing a wide variety of applications, such as antennas, filters and couplers. CST STUDIO SUITE is characterized by its easy-to-use interface, diverse import filters, versatile parameterization capabilities and automatic optimization tools, and includes the powerful post-processing options that get your development process up to speed.

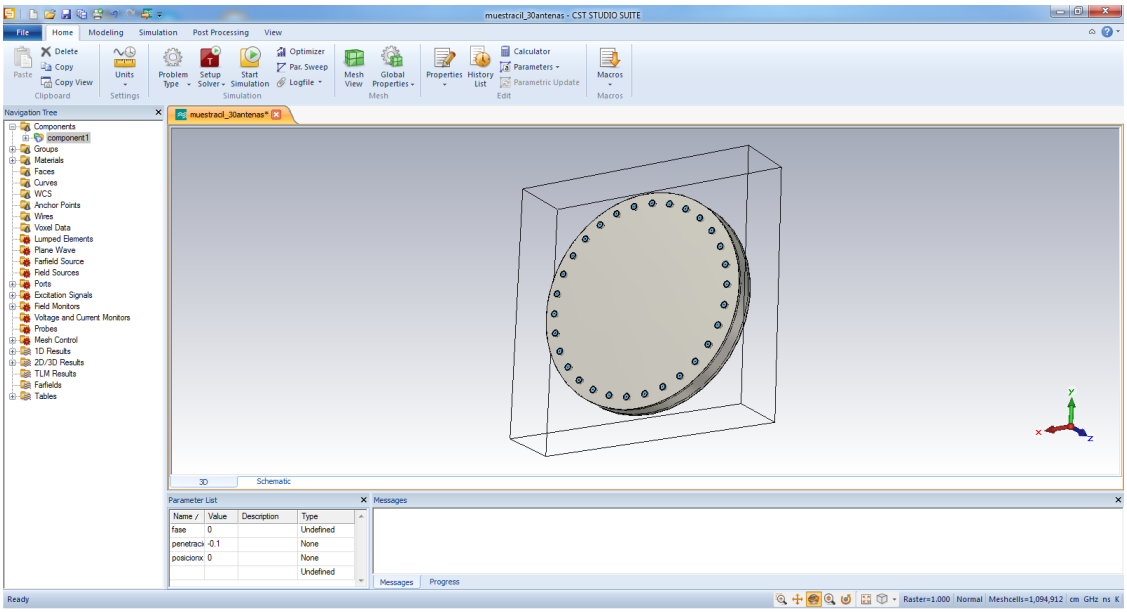

Figure 1.1: CST MWS Interface.

The data obtained after simulating our structure design in CST (total solver time about 3h 42' 56") will be exported to be calculated, painted and illustrated by Matlab. When we compare both results we will demonstrate their similarity and the correct performance of both programs.

Chapter 2

Fundamentals and Related Concepts

In this chapter, different concepts related to this project are being commented, presenting a theoretical point of view about some of them, like Hyperthermia, Array of Antennas and Leaky-wave antennas in order to understand better the marked objectives we want to fulfill.

In the first part of the chapter a brief explanation about Hyperthermia can be found. This fundamental has the purpose to show an important and interesting application of microwaves and has motivated the carrying out of this project from the beginning.

The second part of the chapter deal with the concept of Array of Antennas, which tackles one of the main issues created and developed during this process.

Finally, a good starting point for future work will be proposed, Leaky-wave Antennas, the main subject of this project.

2.1 Hyperthermia: Microwaves as Cancer Treatment

2.1.1 Introduction: Backgrownd

Historically, the treatment of cancer with hyperthermia can be traced back to 3000 B.C. when smouldering sticks of wood were inserted in tumors. At the end of the 19th century, Coley's toxin was introduced to patients to produce whole body hyperthermia which resulted in tumor regression. Over a hundred years ago, doctors first noticed that high heat, such as that resulting from a fever, killed cancer cells and shrank tumors [12].

Research into hyperthermia as a cancer treatment began soon after. During the last decade, especially in recent years, the interest in using hyperthermia and/or in combination with other forms of therapy has increased tremendously [13].

2.1.2 A medical approach

Hyperthermia (or thermotherapy) is a cancer treatment that involves heating tumor cells within the body. Currently, hyperthermia is an experimental treatment in which body tissue is exposed to high temperatures and usually applied to late stage patients. Elevating the temperature of tumor cells results in cell membrane damage, which, in turn, leads to the destruction of the cancer cells. Heating methods include whole body heating using hot wax, hot air, hot water suits, infrared, or partial body heating utilizing radiofrequency (RF), microwave, ultrasound, hot blood, or fluid perfusion [12]. Clinical and experimental results from various countries have indicated a promising future for hyperthermia [13]. By killing cancer cells and damaging proteins and structures within cells, hyperthermia may shrink tumors. However, the main problem is the generation and control of heat in tumors.

The effective temperature range of hyperthermia is very small, 42.5-44°C. At lower temperatures, the effect is very minimum. At temperatures higher than 44°C, the normal cells are damaged [12]. Numerous reports show how various animal or human tumors can be successfully treated by heat alone where high temperatures can damage and kill cancer cells, usually with minimal injury to normal tissues. Also, there are many publications emphasizing how numerous clinical trials have studied hyperthermia in combination with radiation therapy and/or chemotherapy. These studies have focused on the treatment of many types of cancer. Many of these studies, but not all, have shown a significant reduction in tumor size when hyperthermia is combined with other treatments [14–16]. However, not all of these studies have shown increased survival in patients receiving the combined treatments [16].

Tumor temperatures are usually higher than surrounding tissue temperatures during hyperthermia treatment due to the difference in blood flow in normal and tumor tissues. In addition, it is generally believed that tumors are more sensitive to heat. This is explained by the hypoxic, acidic, and poor nutritional state of tumor cells. The synergism of radiation and hyperthermia is accomplished by the thermal killing of hypoxic and S-phase cells which are resistive to radiation. Hyperthermia has been used in combination with chemotherapy, since heating increases the membrane permeability and the potency of some drugs.

2.1.3 Microwave Hyperthermia

Microwave energy is very effective in heating cancerous tumors, because tumors typically have high-water content. Such tissue heats very rapidly when exposed to high-power microwaves. Furthermore, microwaves can be delivered to tissue by special-purpose antennas that are located adjacent to the patient's body. Depending on the tumor size and location in the body, one or more microwave antennas can be used to treat the tumor. When a microwave thermotherapy antenna is turned "on," body tissues with high-water content that are irradiated with significant amounts of microwave energy are heated. The temperature rise in the tissue is due to the transfer of microwave energy into heat. Generating heat from microwaves is very similar to the effect of ordinary mechanical friction such as warming your hands by rubbing them together. As the microwave energy (oscillating about a billion times a second) passes through the tissue, water molecules are vibrated. Frictional forces between the water molecules in the tissue result in the heating of the tissue. By concentrating the microwave energy, it is possible to selectively heat tumors and protect healthy tissues.

The temperature rise in tumors and tissues is determined by the energy deposited and the physiological responses of the patient. When electromagnetic methods are used, the energy deposition is a complex function of frequency, intensity, polarization of the applied fields, geometry, and size of applicator as well as the dielectric property, geometry, size, and depth of the tumor. The final temperature elevations are not only dependent on the energy deposition but also on blood flow and thermal conduction in tissues.

In 1990, Dr. Alan J. Fenn, an electrical engineer at the Massachusetts Institute of Technology's Lincoln Laboratory developed a concept for heating deep tumors by means of adaptive microwaves. These adjust to the properties of a patient's tissue to concentrate the microwave energy at the tumor position. These adaptive microwaves are generated by multiple microwave antennas (*an adaptive phased array*) that surround the human body [17].

Microwaves also show promise as a diagnostic tool, where they will act as a sort of radar for your body. Research in this use of microwaves in medicine, as well as many others, continues. In present hyperthermia research, thermal dosimetry and treatment planning with microwave and RF waves is far from adequate. The cooling mechanism of superficial tissue circulation has made it difficult to heat deep tissue by conductive heating. Diathermy using microwaves, RF waves, and ultrasound is necessary to bring electromagnetic or acoustic energies to tissue beneath the subcutaneous fat layers. Further clinical applications cannot fully proceed without the prerequisite knowledge of how heat is to be delivered in various clinical situations. The development of advanced hyperthermia equipment and techniques will allow successful treatment of cancers that are resistant to other methods of therapy [12].

Microwaves occupy the electromagnetic frequency band between 300 MHz and 300 GHz. The most commonly used frequencies for hyperthermia are 433, 915, and 2450 MHz. They are the designated ISM (industrial, scientific, and medical) frequencies in the U.S. and Europe (433 MHz in Europe only). Frequencies higher than 2450 MHz have no practical value due to their limited penetrations. While RF by definition is between 3 kHz and 300 GHz, generally it means frequencies below microwave range in hyperthermia. The RF frequencies of 13.56 and 27.12 MHz have been widely used in diathermy and now in hyperthermia.

The following heating methods have been used for diathermy in rehabilitation medicine for four decades. During the last ten years, these techniques have been modified and refined for heating tumors.

- **Capacitive Heating**

  Tissues can be heated by displacement currents generated between two capacitor plates. This method is simple, but the overheating of fat remains a major problem. In planar tissue models, the rate of temperature rise is about 17 times greater in fat than in muscle. In addition, the blood flow is significantly less in fat, so the final temperature is much higher than that in muscle.

- **Inductive Heating**

  Magnetic fields generated by solenoidal loops or *"pancake"* magnetic coils induce eddy currents in tissue. Since the induced electric fields are parallel to the tissue interface, heating is maximized in muscle rather than in fat. However, the heating pattern is generally toroidal in shape with a null at the center of the coil.

- **Resistive Heating**

  The operating frequency should be higher than 100 kHz to prevent excitation of nerve action potentials. Tissues can be heated by alternating RF currents through the use of needle or plate electrodes.

- **Radiative Heating**

  The previous three heating methods use frequencies in the RF band where a quasi-static condition applies. In the microwave frequency range, energy is coupled into tissues through waveguides, dipoles, or other radiating devices. The shorter wavelengths of microwaves, as compared to RF, provide the capability to direct and focus the energy into tissues by direct radiation from a small applicator. Loading an applicator with dielectric material can reduce the size of its aperture to provide more flexibility in controlling the amount of energy deposited at tumor sites.

2.1.4 Methods and Clinical Applications

Local Hyperthermia

In local hyperthermia, heat is applied to a small area, such as a tumor, using various techniques that deliver energy to heat the tumor. Different types of energy may be used to apply heat,

including microwave, radiofrequency, and ultrasound. Depending on the tumor location, there are several approaches to local hyperthermia:

1. **Interstitial**

   This approaches are used to treat tumors deep within the body, such as brain tumors. This technique provides better control of heat distributions within the tumor and allows it to be heated to higher temperatures as compared with external hyperthermia. Other advantage includes sparing normal tissue, especially the overlaying skin. Probes or needles are inserted into the tumor under anesthesia. Imaging techniques, such as ultrasound, may be used to make sure the probe is properly positioned within the tumor. The heat source is then inserted into the probe. Radiofrequency ablation (RFA) is a type of interstitial hyperthermia that uses radio waves to heat and kill cancer cells.

   Small microwave antennas inserted into hollow tubings can produce satisfactory heating patterns with frequencies between 300-2450 MHz. A common frequency used in the United States is 915 MHz. A small coaxial antenna can irradiate a volume of approximate 60 cc. With a multinode coaxial antenna, the length of the heating pattern can be extended to about 10 cm in a 3 node antenna [12]. It was calculated the isotherms for an array of antennas taking into account the absorbed power in tissues and relating it to the bio-heat equation. Assumptions with or without blood flow were included in the theoretical modelling.

   The degree of control of microwave power radiating from these antennas is important in order to achieve homogeneous heating. Multiple point feedback control would be important as well.

2. **External**

   This approaches are used to treat tumors that are in or just below the skin. External applicators are positioned around or near the appropriate region, and energy is focused on the tumor to raise its temperature.

   The majority of studies involve the use of microwaves, usually at 915 MHz. In most cases, skin cooling was employed if there was no evidence of superficial tumor [18]. The average complete response rate with irradiation alone is 30 percent in comparison to 70 percent with irradiation and hyperthermia. Toxicities are mainly pain and thermal bums. Side effects of thermal blistering and bums were correlated with maximum temperatures attained during heat treatments.

   A number of microwave applicators with various sizes operate over a frequency range of 300- 1000 MHz. Most of them are dielectrically loaded and with a water bolus for surface cooling. Low profile, lightweight microstrip applicators, which are easier to use clinically,

have also been reported [19]. To reduce the applicator size and weight, methods of using high permittivity dielectric material, electric wall boundary, and magnetic material have been applied. Although these applicators are only useful for treatment of tumors at a few centimeters below the skin, they are much more convenient than waveguide applicators in phased-array applications for treating deep-seated tumors.

3. **Intraluminal or endocavitary**

   This methods may be used to treat tumors within or near body cavities, such as the esophagus or rectum. Probes are placed inside the cavity and inserted into the tumor to deliver energy and heat the area directly.

Regional Hyperthermia

In regional hyperthermia, various approaches may be used to heat large areas of tissue, such as a body cavity, organ, or limb.

To heat deep-seated tumors noninvasively is difficult. RF energy can be deposited into the center of the body but a large region is affected. Differential increases of blood flow in the normal and tumor tissues may result in higher temperature in tumors than normal organs. However, this temperature differential cannot be assured [18].

The annular phased array systems (APAS) consists of four sets of dual radiating apertures which operate in the transverse electromagnetic (TEM) mode over the frequency range of 50-110 MHz [20]. The maximum power is 2 kW. The patient is placed inside the octagonal aperture. Distilled water bolus bags fill the air space within the aperture, and have the function of improving energy coupling, reducing stray radiation, and providing surface cooling. In clinical evaluations, the safety, feasibility, and also the limitations of the use of APAS have been demonstrated for achieving therapeutic temperatures in the abdomen and pelvis. Treatment of the chest can cause severe heating in the head and neck region. In addition, the invasive thermometry current employed can puncture the lung or major vessels [12].

Whole-body Hyperthermia

Whole-body heating is being studied as a way to make chemotherapy work better in treating cancer that has spread (metastatic cancer). Body temperature can be raised by using heating blankets, warm-water immersion (putting the patient in warm water), or thermal chambers (much like large incubators). People getting whole-body hyperthermia are sometimes given sedation (medicine to make them feel calm and sleepy) or even light anesthesia.

A person's body temperature may be raised as if they had a fever, which is sometimes called fever-range whole-body hyperthermia. Studies suggest that this may cause certain immune cells to become more active for the next few hours and raise the levels of cell-killing compounds in the blood. Several studies are testing hyperthermia and chemotherapy along with other treatments that are designed to boost the person's immune system [21].

Phased-Array Hyperthermia

The temperature rise in tumors is determined by the electromagnetic energy deposited in the tissue and the physiological responses of the patient. The energy deposition is in turn a complex function of frequency, intensity and polarization of the applied fields, geometry and size of the applicator, as well as dielectric properties, geometry, size, and depth of the tumor. Single external microwave applicators have been used in combination with water or air-cooling systems to reduce skin temperature and, therefore, can produce deeper therapeutic heating without damage to surface tissues. However, the degree of freedom for manipulation is very limited. Thus, an array of applicators with variations of phase, frequency, amplitude, and orientation of the applied fields can add more dimensions to controlling the heating pattern in tissues [18].

An array of applicators with variations in phase, frequency amplitude, and orientation of the applied fields can add more dimensions to controlling the heating patterns during the treatment. The APAS described by Tuner was composed of 16 synchronized radiating apertures [17]. When the electrical field in the tissue is increased by a factor of N, the specific absorption rate (SAR) (and, therefore, the temperature rise) is N^2 times higher. By changing the phase and amplitude of the applied fields incident from different directions, the SAR pattern can be controlled. Theoretically it is possible to achieve the temperature elevation at the tumor only [12].

the retro-focusing technique was applied to determine the excitation phases of an array for heating an inhomogeneous medium. A small probe was first inserted into a tumor. A signal was radiated from the probe and received by the array of applicators outside the patient. By reciprocity theory, conjugate fields were radiated from the applicators and focused at the tumor [18].

2.2 Conformal Array Antennas

2.2.1 Introduction

Conformal antennas were first introduced in avionics to be integrated with the curve shape of the aircrafts in order to overcome aerodynamic limitations. Nowadays, in order to decrease the physical size of the array antenna or fit it with different shapes, conformal arrays are widely used in various vehicles, high speed trains, satellites, and military surveillance radars. The implementation of some radiation patterns is more accessible using the conformal arrays and they can overcome both physical and radiation patterns restrictions. Shaped beam array antennas are of a great interest in the wireless community.

The key aspect in the design of this type of array antennas is to set the elements excitations including phase and amplitude and the position of array elements to obtain a desired radiation pattern [22]. In recent years, with the emergence of evolutionary optimization methods like genetic algorithms, differential evolution, and particle swarm optimization lots of researches have been carried out for the design of array antennas.

The design and synthesis of an array antenna for a desired radiation pattern is often affected by the mutual coupling effect between its elements. In fact, this effect will cause in a difference between the theoretical synthesis and the practical implementation. In order to consider the far field mutual coupling of the elements in the synthesis process, the complex active radiation pattern of each element in the presence of the other elements must be used [23].

Because of the variation of elements orientation and mutual coupling effect, the radiated fields of elements are different from each other and it must be considered in the array factor equation. So that, the feeding network has an important role in the array antenna design because the resulting radiation pattern and bandwidth of the whole system is highly dependent on it.

2.2.2 Definition

A conformal antenna is an antenna that conforms to a prescribed shape. The shape can be some part of an airplane, high-speed train, or other vehicle. The purpose is to build the antenna so that it becomes integrated with the structure and does not cause extra drag. The purpose can also be that the antenna integration makes the antenna less disturbing, less visible to the human eye; for instance, in an urban environment. A typical additional requirement in modern defense systems is that the antenna not backscatter microwave radiation when illuminated by, for example, an enemy radar transmitter (i.e., it has stealth properties) [23].

The IEEE Standard Definition of Terms for Antennas (IEEE Std 145-1993) gives the following definition:

Conformal antenna (conformal array). An antenna (an array)] that conforms to a surface whose shape is determined by considerations other than electromagnetic; for example, aerodynamic or hydrodynamic.

Usually, a conformal antenna is cylindrical, spherical, or some other shape, with the radiating elements mounted on or integrated into the smoothly curved surface. Many variations exist, though, like approximating the smooth surface by several planar facets. This may be a practical solution in order to simplify the packaging of radiators together with active and passive feeding arrangements.

The need for conformal antennas is pronounced for the large-sized apertures that are necessary for functions like satellite communication and military airborne surveillance radars.

Array antennas with radiating elements on the surface of a cylinder, sphere, or cone, and so on, without the shape being dictated by, for example, aerodynamic or similar reasons, are usually also called conformal arrays. The antennas may have their shape determined by a particular electromagnetic requirement such as antenna beam shape and/or angular coverage. A cylindrical or circular array of elements has a potential of 360° coverage, either with an omnidirectional beam, multiple beams, or a narrow beam that can be steered over 360°.

The arguments for and against conformal arrays can be discussed at length. The applications and requirements are quite variable, leading to different conclusions. In spite of this, and to encourage further discussion, we present a summary based on reflections [18, 23] in Table 2.1.

Parameter	*Planar Array*	*Conformal Array*
Technology	Mature	Not fully established
Analysis tools	Available	In development
Polarization	Sinle can be used (dual often desired)	Polarization control desired (specially if doubly curved)
Beam Control	Phase only usually sufficient, fixed amplitude	Amplitude and phase more complicated
Frequency Bandwidth	Tipically 20%	Wider than planar
Gain	Drops with increased scan	Controlled, depends on shape
RCS	Large specular RCS	Lower than planar
Angular Coverage	Limited to roughly +-60º	Very wide, half sphere
Radome	Aberration effects	No conventional radome, no boresight error
Instalation of Platform	Planar shape limits due to swept volume	Structurally integrated. Leaves extra space, no drag
Packgaging of Electronics	Known multilayer solutions	Size restriction if large curvature, facets possible

Table 2.1: Planar vs. Conformal Array Antennas.

With this comparison, some differences between planar and circular arrays can be understood to enhance arrays knowledge. Depending on their characteristics, it will be easier choosing the correct design to obtain the best possible performance.

2.2.3 History

The field of phased array antennas was a very active area of research in the years from WW II up to about 1975. During this period, much pioneering work was done also for conformal arrays. However, electronically scanned, phased array antennas did not find widespread use until the necessary means for feeding and steering the array became available.

Digital processing techniques made phased array antenna systems cost effective, that is, they provided the customers value for the money spent. This being true for phased arrays in general, it also holds for conformal array antennas. However, in the area of conformal arrays, electromagnetic models and design know-how needed extra development. During the last 10 to 20 years, numerical techniques, electromagnetic analysis methods, and the understanding of antennas on curved surfaces have improved. Important progress has been made in high-frequency techniques, including analysis of surface wave diffraction and modeling of radiating sources on curved surfaces.

The origin of conformal arrays can be traced at least back to the 1930s when a system of dipole elements arranged on a circle, thus forming a circular array. The circular array was attractive because of its rotational symmetry. Proper phasing can create a directional beam, which can be scanned 360° in azimuth. The applications were in broadcasting, communication, and later also navigation and direction finding.

2.2.4 Near-Field-Focused Antennas

Near-field-focused (NFF) antennas have been studied over a long time. The basic idea is to control the phase of the radiation sources on the antenna's aperture (the array-element currents or equivalent surface currents) in such a way that all their contributions sum in phase at a specific focal point, located in the antenna's near-field region. However, their applications are limited in number when compared to antennas for communication systems and radars, which are generally focused in the antenna's far-field region [3].

Specifically, for near-field-focused antennas, a maximum of the radiated field is obtained in the vicinity of the above focal point (actually, the power-density peak is placed between the focal point and the antenna's aperture). This is obtained by implementing a symmetric source-phase tapering, capable of compensating for the different distances between each source point on the aperture and the focal point. The result is that for a given amplitude of the radiated field at a point in the far-field region, such as, for example, the amplitude value that can be derived from the maximum EIRP (Effective Isotropic Radiated Power) allowed by international safety standards and regulations, the peak power density given from the near-field-focused antenna will be greater than that obtained from the corresponding far-field focused antenna (equal-phase antenna).

Near-field-focused antennas have been applied in several areas, such as local hyperthermia and imaging systems, both in biomedical and in industrial microwave applications.Design and performance curves are given as functions of the array size, the inter-element distance, and the focal distance. Near-field-focused antennas can be realized by pyramidal or conical horns, by resorting to a lens in front of the antenna aperture.

Alternative solutions are based on either reflector antennas or Fresnel-zone antennas. On the other hand, lightweight, low-profile, as well as low-cost near-field-focused antennas can be obtained by using planar microstrip arrays, with a feeding network exhibiting relatively small differences with respect to a corporate feeding network of a conventional far-field focused array. While most previous work on near-field-focused planar arrays (such as those, for instance, relevant to non-contact microwave inspection [2] and temperature monitoring [4]) were relevant to microstrip arrays operating at frequencies greater than 10 GHz. More recently, near-field-focused microstrip arrays have been designed and characterized at relatively lower frequencies (1.8 GHz and 2.4 GHz), to be used in systems for gate-access control and management [3].

2.2.5 Circular Array Theory

The circular array antenna can be seen as an elementary building block of conformal array antennas with rotational symmetry, just as the linear array is a building block of planar array antennas. By studying circular arrays we can understand some basic aspects of conformal array antennas, especially cylindrical and conical arrays and other shapes with rotational symmetry.

The term "ring array" is sometimes used instead of "circular array" to distinguish it from a circular area filled with radiating elements, which is a circular *planar* array antenna (Figure 2.1(a)). We use the term circular array here, however, to mean an array of radiators distributed with equal spacing along the periphery of a circle, as in Figure 2.1(b).

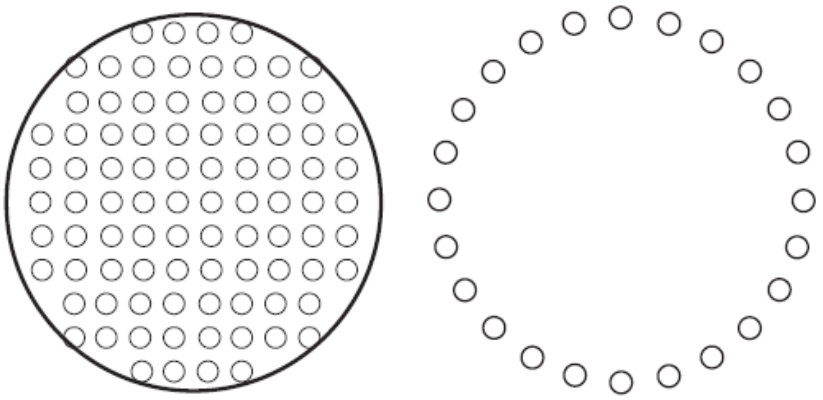

(a) Circular Planar Array (b) Circular Ring Array

Figure 2.1: Comparison of Circular Arrays.

Circular array antennas with uniformly spaced radiating elements and with equal amplitude and phase excitation have long been used for the purpose of obtaining good omnidirectional patterns in the plane of the array (usually the horizontal plane). Later applications include phase-steered directional beams and arrays with several simultaneous beams, including broadband circular arrays. A linear variation of phase along the array circumference was analyzed in the 1930s. He demonstrated that a reduction in the elevation beamwidth and, consequently, a concentration of the radiation in the horizontal plane could be achieved with

this phasing arrangement, while still preserving an omnidirectional amplitude pattern in the azimuth. This was expected to reduce fading in communication systems, since the interference between a ground wave and signals reflected from the ionosphere was reduced, resulting in an "antifading antenna". In fact, the concept *phase mode* was introduced. Phase mode theory was later used as an efficient tool for the understanding of the behavior of circular arrays and for pattern synthesis and the use of directional elements has been shown to considerably improve the circular array pattern bandwidth compared to using isotropic elements.

This generic array has elements equally spaced along the periphery of a circle (Figure2.2), and the elements are excited with equal phase and amplitude.

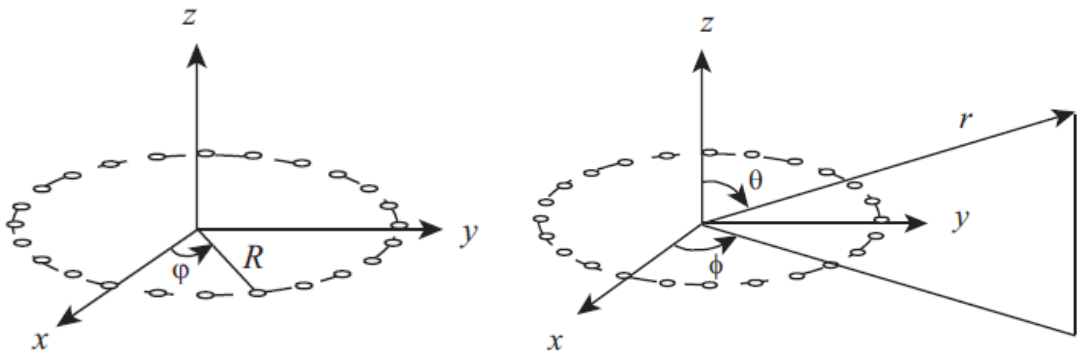

(a) Local coordinates (b) Far-field coordinates

Figure 2.2: Cordinates for the Circular Array.

We will start by an analysis of the radiation in the plane that contains the array, which we refer to as the azimuth (or horizontal) plane. Local coordinates on the circle are (R, φ), the radius and angle, respectively (Figure 2.2 (a)). Far-field coordinates are indicated by (r, θ, ϕ) (Figure 2.2 (b)). We will neglect mutual coupling effects, that is, we consider element excitations (voltages or currents) as given or specified including the effects of mutual coupling. Limiting the analysis to the azimuth plane only makes the circular array problem a two-dimensional problem, that is, it has bearing on other two-dimensional problems like cylindrical array structures.

The corresponding far-field expression for the circular array (Figure 2.3 (b)), in the azimuth plane is

$$E(\phi) = \sum_n V_n EL(\phi - n\Delta\varphi) e^{jkR(cos(\phi - n\Delta\varphi))} \tag{2.2.1}$$

where the phase has been referenced to the center of the circle. V_n is the excitation amplitude of element n and k is the propagation constant, $k = 2\pi/\lambda$. The identical elements are spaced $R\Delta\varphi$ along the circle, each element pointing in the radial direction. The element function can, therefore, in general not be brought outside the summation, since it is a function of the element position; there is no common element factor $EL(\phi)$. The radiation function is

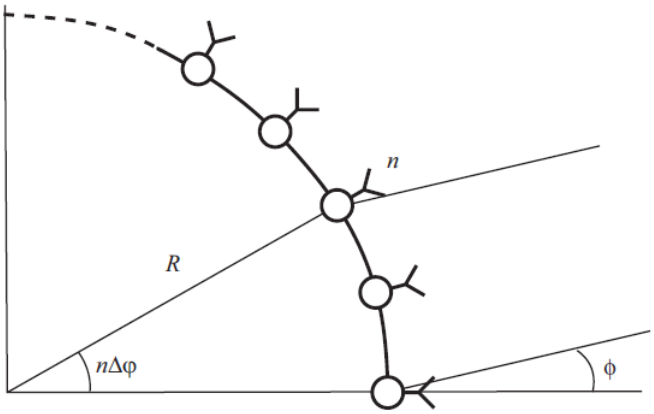

Figure 2.3: Part of a Circular Array.

the product of the element factor and the array factor but with dropped vector signs (overbar) to simplify notation. Consequently, we can, in general, not define an array factor, unless the elements are isotropic, that is, have isotropic (omnidirectional) radiation at least in the horizontal plane. A typical example of the latter is an array of vertical dipoles with their axes perpendicular to the array plane.

With the circular array, we can impose phase values to each element so that they add up coherently in the direction ϕ_0. We get the proper phase excitation (beam cophasal excitation) for each element n by choosing

$$\psi(n) = -kRcos(\phi_0 - n\Delta\varphi) \tag{2.2.2}$$

Thus, the radiation function for the focused, circular case becomes

$$E(\phi) = \sum_n |V_n| EL(\phi - n\Delta\varphi) e^{jkR[cos(\phi - n\Delta\varphi) - cos(\phi_0 - n\Delta\varphi)]} \tag{2.2.3}$$

Sometimes, it is required to generate a beam with equal radiation in all directions in the azimuthal plane (an omnidirectional beam). Circular arrays are particularly suitable for this by virtue of their circular symmetry.

2.3 Leaky-Wave Antennas

2.3.1 Introduction

Millimeter waveguides, such as coplanar lines, microstrip lines and dielectric guides, are open structures where energy leakage is bound to occur. This leakage can occur, for example, when there are discontinuities in the guiding structure, or perhaps when the guide is excited in an inappropriate mode. In terms of antenna design, this energy leakage may be advantageous and exploited. This is accomplished through intentionally creating discontinuities in the guiding structure in such a manner that the radiation produced is controlled by the antenna designer. These antennas are very suitable for integrated designs, seeing that they are compatible with the waveguides from which they are derived, essentially limiting the unwanted and imperfect transitions between guiding media. This property also eliminates the requirement for complex and lossy feed networks present in other types of planar structures [24].

That is the reason why *Leaky-wave antennas* have received much attention in the recent years for applications in the millimeter-wave ranges. In particular, the compatibility with printed circuit board technology, their low profile, easiness of fabrication and integration with other planar components are the strongest features of these antennas.

The analytical work on this class of antennas has been limited mainly to evaluation of the leaky-mode propagation constants as a function of the geometrical parameters. From a knowledge of the leaky-mode eigenvalue and its dependence on geometrical parameters, the attenuation constant along the antenna can be designed to give the aperture distribution that will yield the desired radiation pattern. The aperture distribution is assumed to be governed only by the power input at the antenna input and the attenuation constant along the antenna. Although an aperture distribution calculated on the above assumption is only approximate it still yields a pattern in good agreement with experimental measurements.

2.3.2 A brief Definition

Leaky-wave antennas belong to the travelling wave antenna class. Travelling wave antennas are characterized by a simple feed launching one or more travelling wave modes in a guiding structure [25]. The modes launched in the guiding structure can be classified as "*slow*" or "*fast*", if their phase velocity is respectively lower or higher than the free space velocity. Surface wave antennas and slot arrays are also part of the travelling wave family, where surface waves are examples of slow waves, whereas leaky waves are examples of fast waves. While they share some defining features, their performance expectations and design methodologies differ. The modes travelling in the guiding structure control the field distribution on the radiating aperture of the antenna and then the radiation mechanism associated to the antenna.

On the other hand, travelling wave antennas that support surface waves, like surface wave antennas, radiate power flow from discontinuities in the structure that interrupt the bound wave on the antenna surface. The different radiation mechanism has direct effect on the mismatch problems of the two structures.

Focusing on the leaky-wave antennas, it is worth noting that the leaky mode is normally a small degradation of the feeding mode coming from the feed and then no mismatch problems are found at this point [26]. Moreover, as already addressed introducing the radiation mechanism of these antennas, the leaky mode leaks power travelling along the structure and then an insignificant amount of power is left by the time the wave reaches the end of the structure. Even if reflected, this vestigial power cannot cause any serious mismatch problem. Consequently normally leaky-wave antennas, if adequately fed, do not present any mismatch problem, in contrast with the case of surface wave antennas where both the feed and the end termination can pose serious design problems.

Mathematically, a leaky wave is treated as a guided complex wave and the resulting radiation pattern is characterized by a complex propagation constant $k_t = \beta_t - j\alpha_t$ with $|\beta_t|$ lower than k_0, the free space propagation constant. The leaky-wave mode then travels in the guiding structure faster than the speed of the light and at the same time it leaks energy in reason of the attenuation constant α_t [27]. In the lossless case, this energy is totally radiated by the structure and so the leaky-mode couples the guided power into free space.

As a subset of travelling wave antennas, leaky-wave antennas are further divisible into two categories, namely one-dimensional and two-dimensional variants. Similar to other travelling wave antennas, leaky-wave antennas radiate primarily in the endfire direction, but they are very suitable for frequency scanning and as such are often implemented for this purpose.

2.3.3 Contextualization

In order to accomplish this project, some research has been presented in this section as a future line of investigation about this issue.

1. For instance, related to the concepts established in this work, we will analyze the concept of *Conformal Tapered Leaky-wave Antennas* [9], where the theory proposed predicts the distortion in the radiation pattern (deviation of the scanning angle and loss of directivity) due to the curvature of the antenna. This leads to the necessity to taper the leaky mode in order to correct for the curvature [28–30], so that the directive beam pointing at the desired scanning angle is recovered. A simple and accurate design expression was derived with that purpose. To restore the desired narrow beam pointing at the required scanning angle, the LWA must be tapered, therefore, the developed theory was applied to the analysis and design of a conformal leaky-wave antenna in hybrid technology. The simulated radiated patterns showed excellent agreement with leaky-mode theory, validating the proposed analysis and design technique.

   At the end, this novel theory provided an efficient and general tool to analyze curved LWAs and to systematically design tapered conformal leaky-wave antennas that maintain their desired high-directive scanning performance in spite of their curved shape.

2. Another interesting example would be that one which offers a controllable transversely polarized *Leaky wave Applicator based on an Array of Asymmetric Troughguide Antennas* to be involved with cancer therapy by using localized hyperthermia [31]. As a bound-mode structure, the radiation characteristics were weakly affected by lossy tissue loading. This applicator could be designed to closely simulate the theoretically optimal cylindrical configuration.

   In many ways, this antenna was an improvement over currently used applicators. It has most of the advantages of microwave horns without the necessity of dielectric loading. The troughguide is an electrically flexible linear array, and thus simplifies the power-splitting and phase-shifting feed network. It also has a novel non-perturbing power monitoring capability. With all these advantages, the troughguide appears to be a good candidate for a microwave hyperthermia applicator.

3. In *Unusual Tapering of Leaky-wave Radiators* [8], leaky- wave modes must be tapered to enhace the performance of leaky-wave radiators in order to control the amplitud and phase of the radiated fields, with the final objective to tailor the far-field radiation diagram of the near-fields power distributions and improve the performance of the antenna compared to the nontapered counterpart. In this way, leaky-wave antennas with flexible control over the scanning angle, main beam width rejection level out from the prescribed beam, and insertion of radiation nulls should be designed. Also, the near fields can be tailored to obtain focal region where the energy is concentrated, conceiving leaky-wave lenses.

   Moreover, the unusual tapering technique are extensible to CLWA and LW lenses, while keeping their respective far-field and near-field focusing properties where is required an unusual simultaneous tapering of the leaky-wave leakage rate and pointing angle along the leaky radiator.

There are several papers which also refer to this concept as [6,7,10], etc. It was fundamental providing context for that issue since it will be our first starting point to keep developing this idea of creating heating patterns while improving other disturbing areas of the phased array of antennas. In conclusion section it will be explained in depth the proposed design and its characteristics.

Chapter 3

Structure Design

This chapter presents the initial structure design we have worked with and its features. Subsequently, this structure will be optimized to achieve different results and the desired goals.

Figure 3.1 represents the structure which consist of a cylindrical wet clay sample covered by a cylindrical metallic cavity (Microwave Oven) excited by several coaxial antennas.

As we are working in the microwave range, the operating frequency f_o is 2.45 GHz.

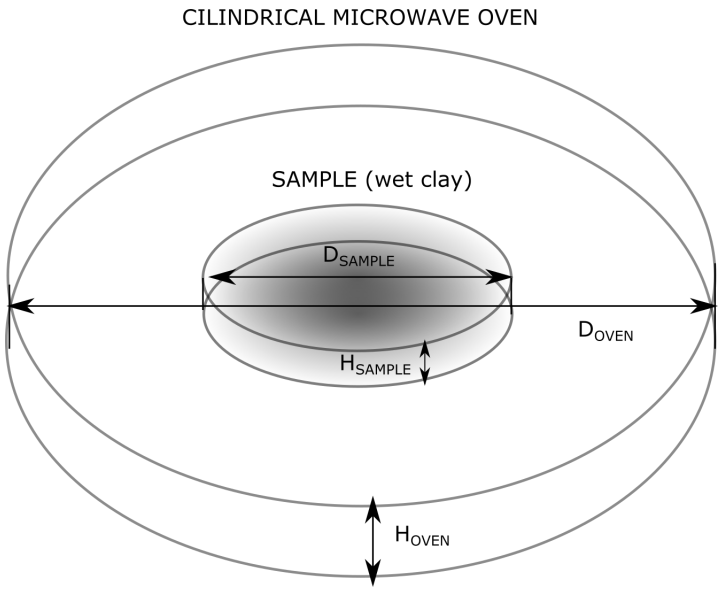

Figure 3.1: Cylindrical microwave oven with cylindrical sample.

The cavity is excited by 30 monopole antennas as shown in Figure 3.2 (b) in a top view. Figure 3.2 (a) shows a CST model of the overall system.

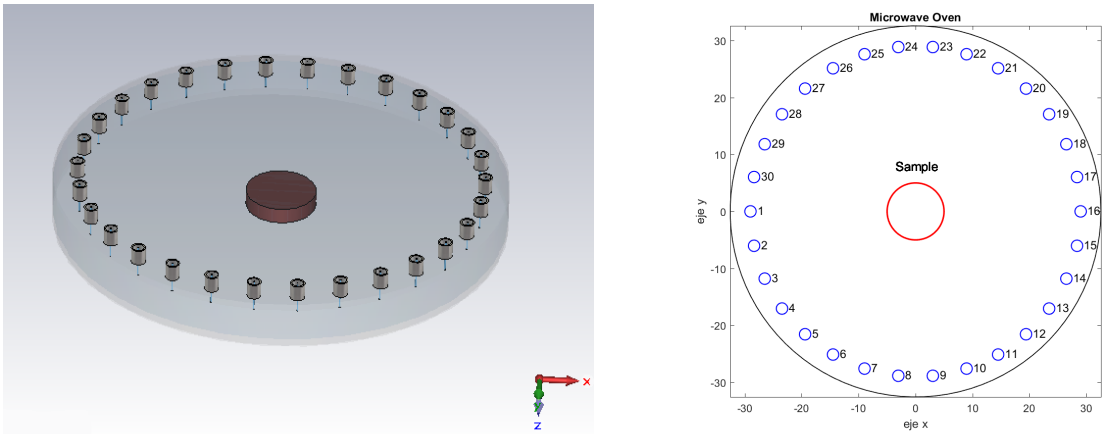

(a) CST Structure Design

(b) Matlab Structure Design

Figure 3.2: Simulation Structure in CST and Matlab.

3.1 Cylindrical Sample

This *wet clay* sample have the following dimensions: La muestra de arcilla mojada (wet clay) posee las siguientes dimensiones:

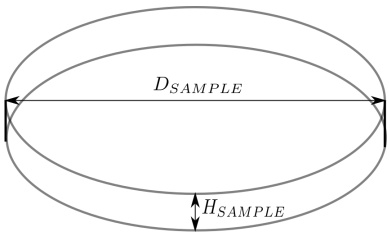

Figure 3.3: Cylindrical Sample.

- D_{SAMPLE}= 10 cm
- H_{SAMPLE}= 2 cm
- Wet Clay properties:
  - $\epsilon_r = 30$
  - $tg\delta = \frac{5}{30} = \frac{1}{6} = 0.16$

3.2 Coaxial Antenna

This figure illustrates a side view to define the coaxial monopole location and associated dimensions:

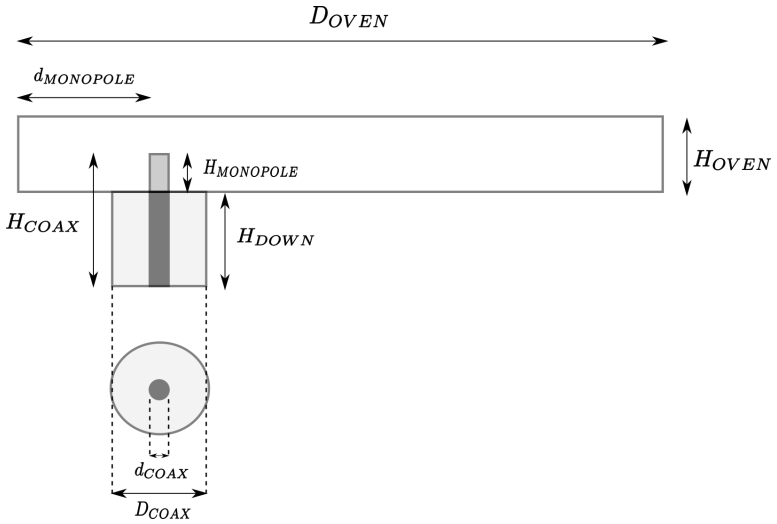

Figure 3.4: Coaxial Antenna.

A standard BNC connector determines the coaxial feeding size.

- D_{COAX}= 2 cm
- d_{COAX}= 0.2 cm
- $\epsilon_{r_{COAX}} = 1$
- H_{COAX}= 1.2665 cm
- H_{DOWN}= 1.0665 cm
- $H_{MONOPOLE}$= 0.2 cm
- $d_{MONOPOLE}$= 3.56 cm

The monopole height and position, $H_{MONOPOLE}$ and $d_{MONOPOLE}$, have been optimized to provide good input matching at the design frequency of 2.45GHz.

Figure 3.5 shows the obtained input matching with CST after optimization, in the presence of a single monopole antenna so that, no coupling can occur with other antennas waveports. Return losses below -60dB are obtained, thus assuring good coupling to the cavity and efficient transfer of energy to the lossy sample. We have to take into account that the sample has also been chosen of cylindrical shape to keep the symmetry of the whole system.

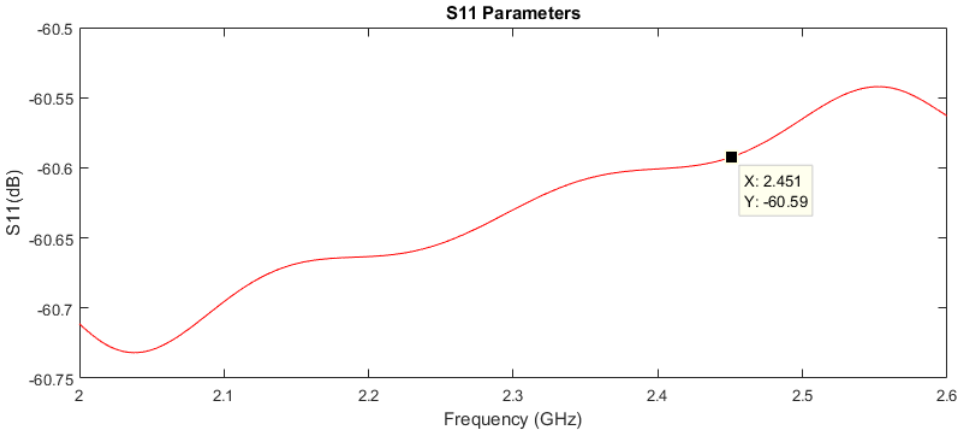

Figure 3.5: S_{11} parameters with $D_{OVEN} = 65.12$ cm.

Furthermore, in free space conditions the antennas dimensions, or in this case, the coaxial antennas measurements should be:

$$H_{MONOPOLE} = d_{MONOPOLE} = \frac{\lambda}{4} = \frac{\frac{c}{f_o}}{4} = 3.06 \text{ cm}$$

As it can be seen, $d_{MONOPOLE} = 3.56 \simeq 3$ cm, however, $H_{MONOPOLE}$= 0.2. The reason is that in cavities theory, the antenna is not considered as such, but rather as a coupling circuit. Thus, its optimum dimension depends on the cavity impedance itself, which makes the monopole heigth less than $\lambda/4$ in some cases [32].

3.3 Cylindrical Cavity (MICROWAVE OVEN)

The microwave oven design consist of a *PEC* cavity with interior *vacuum*, resulting:

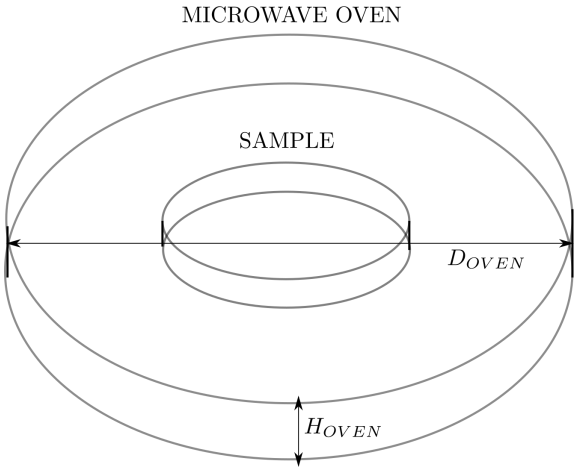

Figure 3.6: Cylindrical cavity (MICROWAVE OVEN).

- H_{OVEN}= 6.17 cm

  - To avoid modes propagation, only TE_{011} mode. Moreover, $H_{OVEN} < \frac{\lambda_0}{2} = 6.122$ cm because of the fundamental mode TE_{010}.

    Using the Resonant Frequency Equation [33]:

$$f_{nlq} = \frac{1}{2\pi\sqrt{\mu\varepsilon}}\sqrt{\left(\frac{\rho'_{nl}}{a}\right)^2 + \left(\frac{q\pi}{d}\right)^2} \tag{3.3.1}$$

    In the TE_{011} mode, we want to obtain d which is H_{OVEN}. It is known that $\rho'_{01} = 3.832$, $a = 30$ cm (default cavity radius) and the Resonant Frequency is 2.45 GHz.

$$f_{011} = \frac{1}{2\pi\sqrt{\mu\varepsilon}}\sqrt{\left(\frac{\rho'_{01}}{a}\right)^2 + \left(\frac{q\pi}{d}\right)^2} = \frac{c}{2\pi}\sqrt{\left(\frac{\rho'_{01}}{a}\right)^2 + \left(\frac{\pi}{d}\right)^2}$$

$$2.45 \cdot 10^9 = \frac{3 \cdot 10^8}{2\pi}\sqrt{\left(\frac{3.832}{30 \cdot 10^{-2}}\right)^2 + \left(\frac{\pi}{d}\right)^2}$$

$$51.31268 = \sqrt{\left(\frac{3.832}{30 \cdot 10^{-2}}\right)^2 + \left(\frac{\pi}{d}\right)^2}$$

$$(51.31268)^2 = \left(\frac{3.832}{30 \cdot 10^{-2}}\right)^2 + \left(\frac{\pi}{d}\right)^2$$

$$(51.31268)^2 = 163.158 + \frac{\pi^2}{d^2}$$

$$d = \sqrt{\frac{\pi^2}{2595.085}} = \frac{\pi}{50.94} = 6.167cm \tag{3.3.2}$$

- D_{OVEN}= 65.12 cm

  - OR=32.56 cm obtained after an oven cavity radius optimization by a radius sweep $R_{OVEN} = [15 - 35]$ cm to achieve $S_{11} < -10dB$ at the resonant frequency $f_0 = 2.45GHz$ and to assure a good electric field concentration in the sample using an exciting coaxial antenna.

Chapter 4

Results

This chapter presents the results of the electric fields created by each one of the individual antennas obtained with CST whose data are extracted to be processed with Matlab. They show the figures represented when only a single antenna is exciting the oven, as well as several combinations of antennas create different heating distributions to further comment.

4.1 Simulations with a Single Antenna

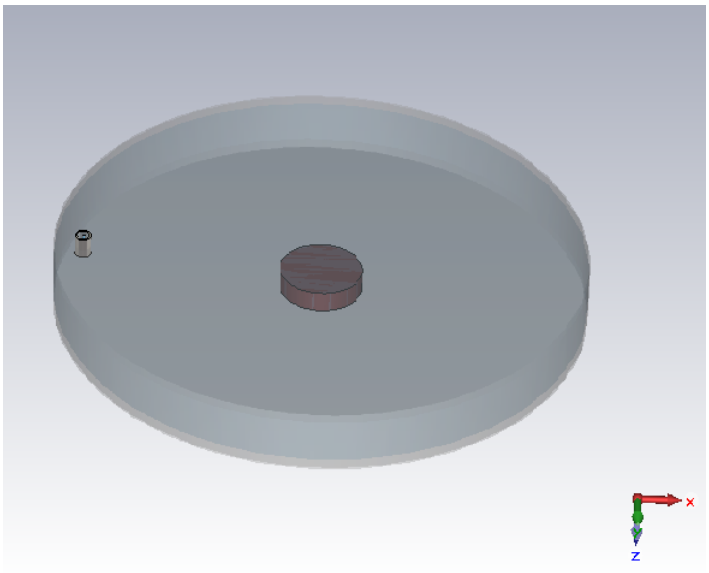

Figure 4.1: Single Antenna Structure.

Figure 4.2(a) shows the transverse E-field intensity pattern when antenna number 1 is excited (Figure 4.2(d)). As it can be seen, the transverse field component is evanescent and the stored energy is concentrated around the antenna. On the contrary, the normal component of the electric field (Ez according to the axes in Figure 4.1) is propagative, generating the field pattern represented in Figure 4.2(b).

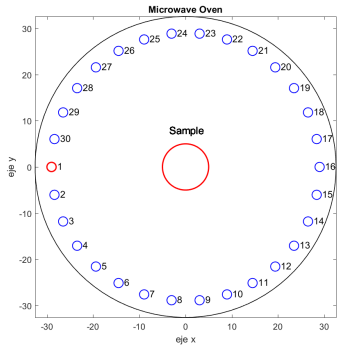

(a) Antenna 1

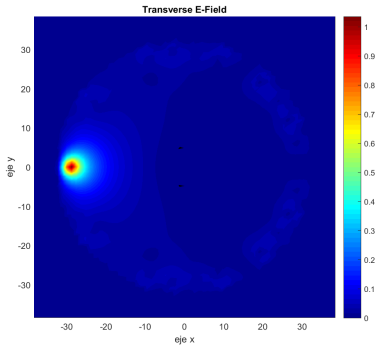

(b) Transverse E-Field E_t

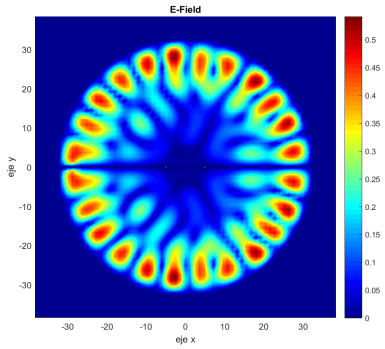

(c) Normal E-Field E_z

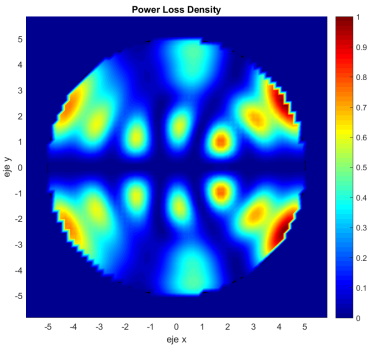

(d) Power Loss Density in the region of sample

Figure 4.2: Field intensity pattern when only antenna 1 is excited.

Therefore, only the z-component of the electric field generated by the antenna propagates and reaches the sample. Using the following well-known heating equation (4.1.1) , the power loss inside the sample can be computed from the electric field intensity inside the sample $E_{z_{SAMPLE}}(x, y)$ and the sample loss factor ε_r'' for the frequency of analysis [34]:

$$P_{LOSS}(x, y) = \omega \varepsilon_r'' \varepsilon_0 |E_{z_{SAMPLE}}(x, y)|^2 \tag{4.1.1}$$

Figure 4.2(c) represents the normalized power loss density in a zoomed region around the sample (area of $6 \times 6\ cm^2$), showing the heating pattern inside the sample associated to the excitation of antenna 1. This power loss pattern shows an uneven heating distribution when antenna 1 excites the microwave oven.

Furthermore, it has to be illustrated that all the patterns drawn by Matlab are very similar to the representation given by CST, so there is no doubt of the proper system operation. On the next page, in figure 4.3, it can be seen how Electric Field, Power Flow (Poynting Vector) and Power Loss Density of antenna 1 follow the same distribution although in some cases, maximums and minimums are clearer using CST.

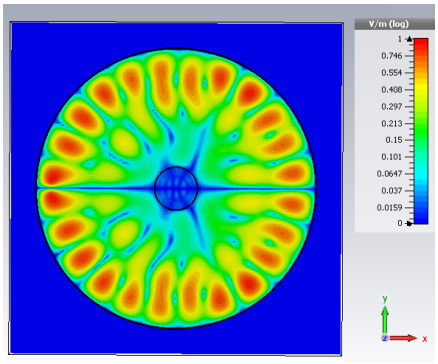

(a) CST Electric Field

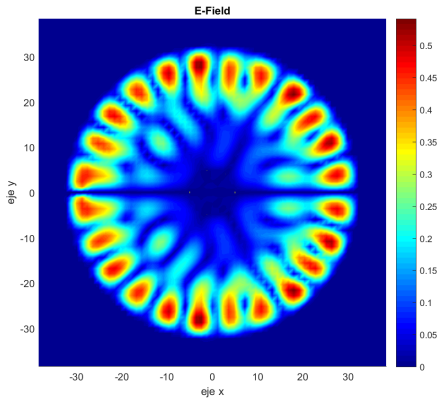

(b) Matlab Electric Field

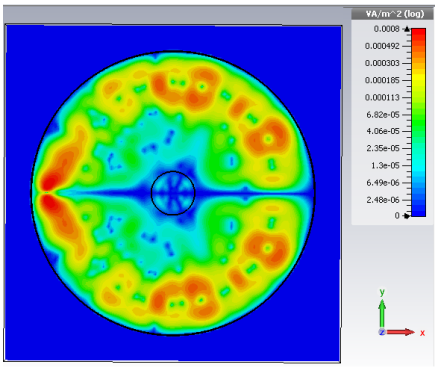

(c) CST Poynting Vector

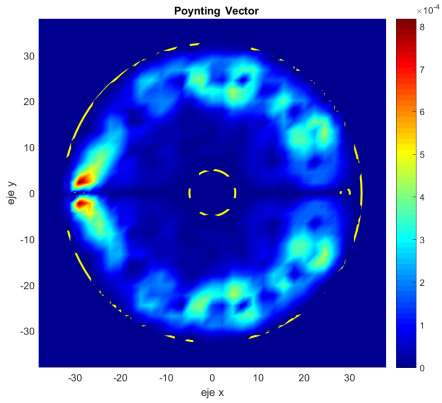

(d) Matlab Poynting Vector

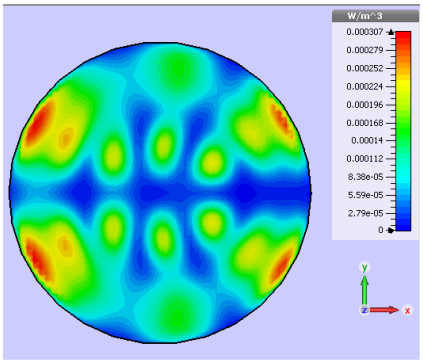

(e) CST P_{LOSS} Density

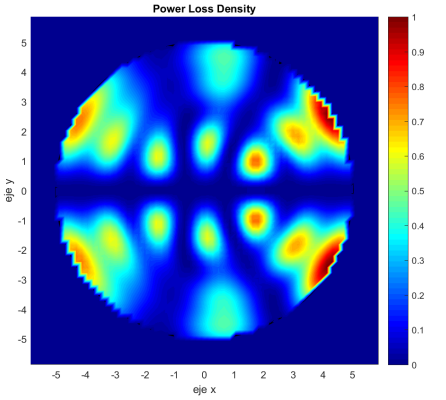

(f) Matlab CST P_{LOSS} Density

Figure 4.3: Comparison of the power loss density with CST and Matlab when Antenna 1 is exciting the oven.

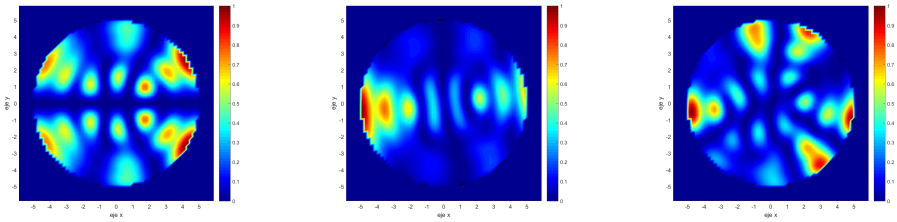

(a) Antenna 1 (b) Antenna 2 (c) Antenna 3

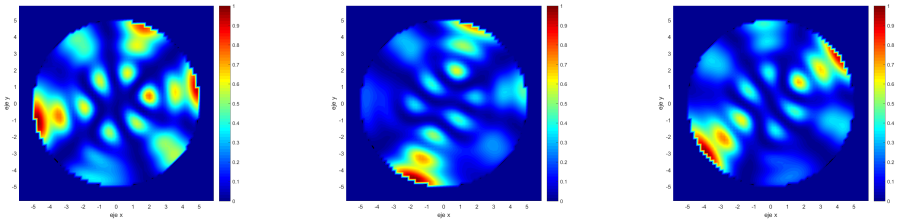

(d) Antenna 4 (e) Antenna 5 (f) Antenna 6

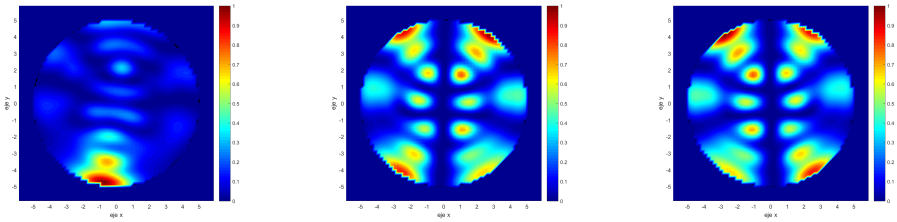

(g) Antenna 7 (h) Antenna 8 (i) Antenna 9

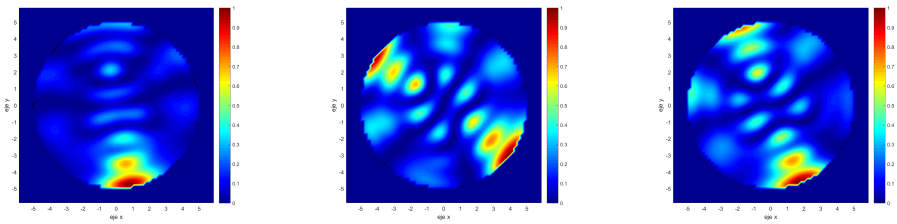

(j) Antenna 10 (k) Antenna 11 (l) Antenna 12

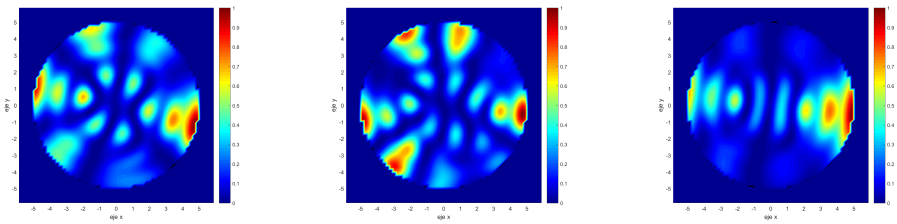

(m) Antenna 13 (n) Antenna 14 (o) Antenna 15

Figure 4.4: Power Loss Density (Antenna 1-15)

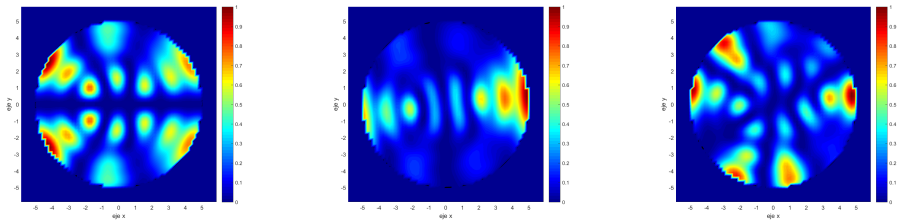

(a) Antenna 16 (b) Antenna 17 (c) Antenna 18

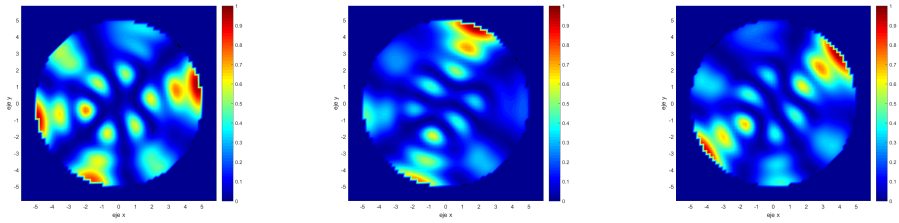

(d) Antenna 19 (e) Antenna 20 (f) Antenna 21

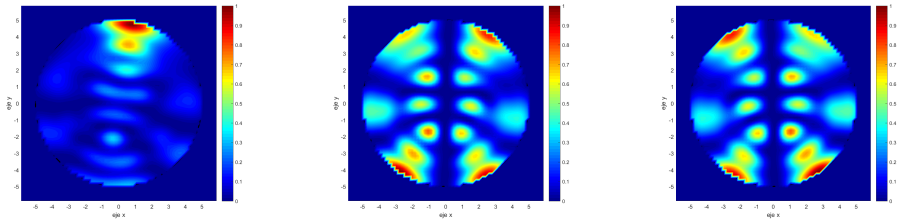

(g) Antenna 22 (h) Antenna 23 (i) Antenna 24

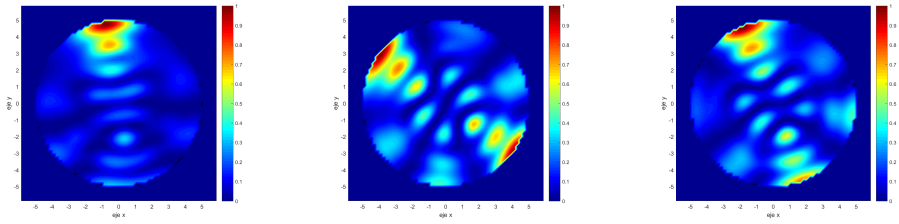

(j) Antenna 25 (k) Antenna 26 (l) Antenna 27

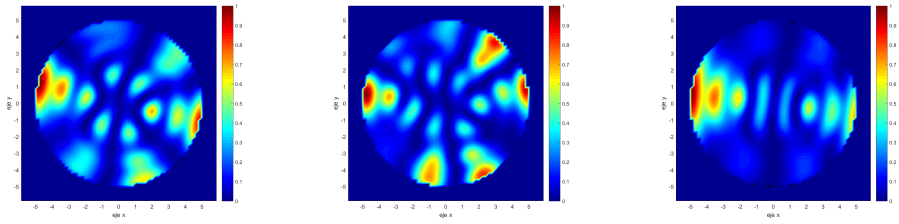

(m) Antenna 28 (n) Antenna 29 (o) Antenna 30

Figure 4.5: Power Loss Density (Antenna 16-30)

Different heating spatial distributions inside the sample are obtained when other antennas are used to feed the oven, as shown in Figure 4.4 and 4.5.

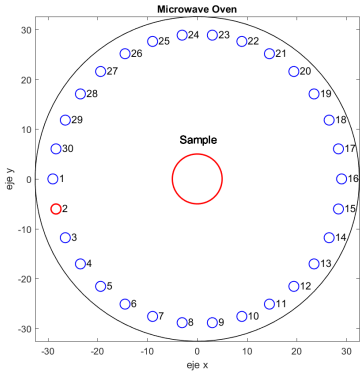

(a) Antenna 2

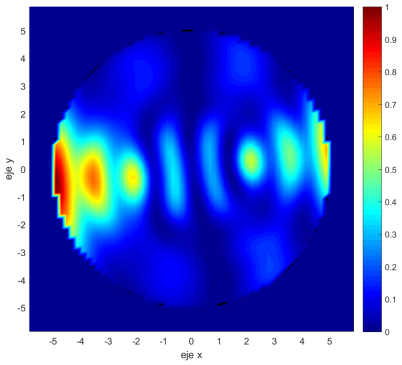

(b) Antenna 2 Pattern

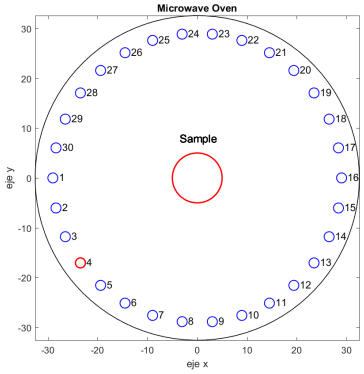

(c) Antenna 4

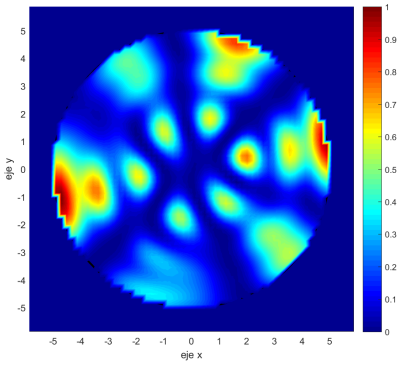

(d) Antenna 4 Pattern

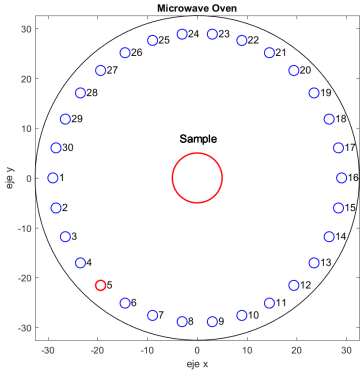

(e) Antenna 5

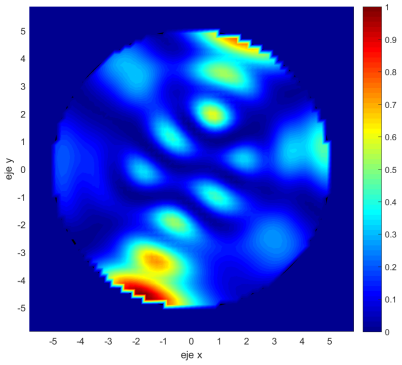

(f) Antenna 5 Pattern

Figure 4.6: Power loss Distribution of different Antennas

The power loss patterns are quite different when comparing the power distributions for antenna 1 in Figure 4.2(d) with those for antenna 2, 4 and 5 in Figure 4.6(a,b,c), respectively.

Nevertheless, he differences between some of the heating patterns are mainly due to rotation created by the azimuthal symmetry of the antennas location and the oven and sample cylindrical shapes (chosen like this to precisely assure that symmetry).

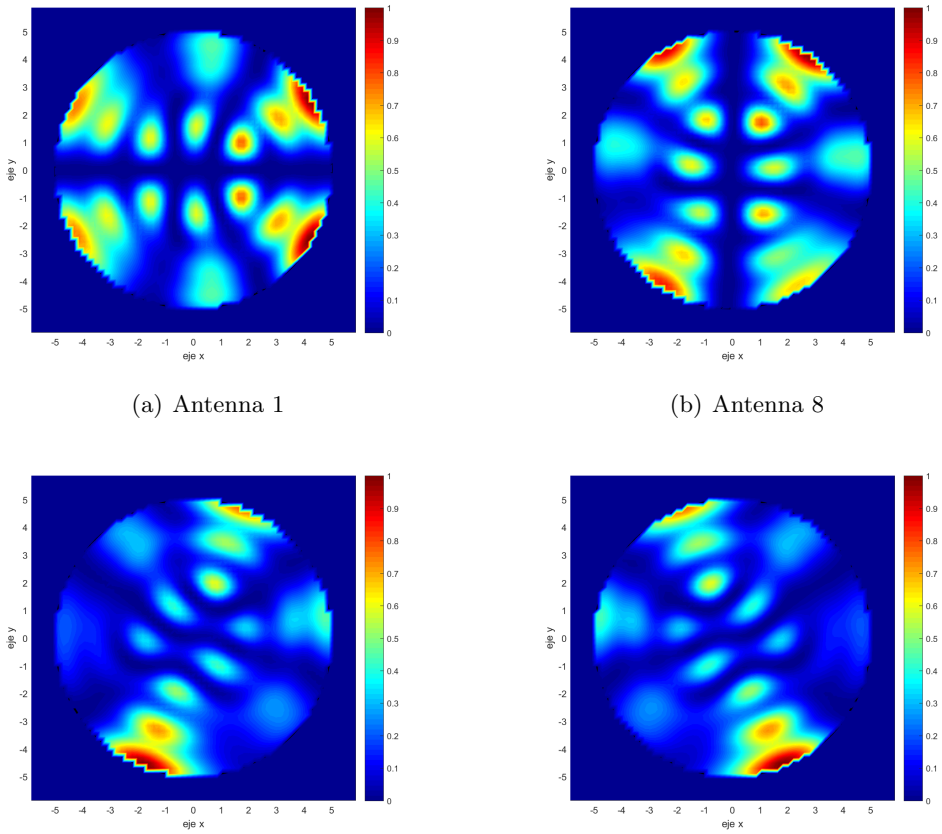

(a) Antenna 1

(b) Antenna 8

(c) Antenna 5

(d) Antenna 12

Figure 4.7: Symmetry between pairs of antennas

For instance, in the present figure if we take a closer view, the heating pattern for antenna 8 (Figure 4.7(b)), is similar to the one of antenna 1 (Figure 4.7(a)) but rotated 90º as it corresponds to the relative positions of antennas 1 and 8 (Figure 3.2). Again, the power loss density pattern for antennas 5 and 12 have similar but rotated distributions. Overall, looking at the Figure 4.4 and 4.5 we will notice that antennas 16-30 (the second figure) presents even the same patterns as in first (antennas 1-15), but with a 180º rotation.

4.2 Combination of Antennas

Now, we are going to discuss different cases when several antennas at the same time feed the oven, an the different distribution presented depending on the antennas and their characteristics.

So that, if several antennas are excited at the same time, each one with a complex weight C_i (with $i = 1 \dots 30$), which represents the amplitude and phase of each antenna ($C_i = A_{i_{\phi_i}} = A_i \exp^{j\phi_i}$), the resulting electric field inside the sample is created by the complex interference of each individual field, multiplied by the weight C_i :

$$E_{TOTAL_{SAMPLE}}(x,y) = \sum_{i=1}^{30} C_i \cdot E_{i_{z_{SAMPLE}}}(x,y) \tag{4.2.1}$$

Using this total field in equation 4.2.1, the heating pattern due to power loss density inside the sample can be computed for any combination of excitations in the proposed phased-array microwave oven with the previous equation 4.1.1.

The following table describes different combination of antennas with different weights C_i in order to create pattern shapes as uniformly as possible. In spite of the existence of multiple combinations (so it is impossible to test all of them), in this table, only some examples are summarized in order to discover how synthesize an algorithm to create patterns in the future.

CASE	*Excitation vector* C_i
A	$C_i = 1_{0^o}$ for all antennas $i = 1...30$
B	$C_1 = 1_{30^o}$, $C_5 = 0.7_{-45^o}$
C	$C_1 = 1_{180^o}$, $C_2 = 1_{45^o}$, $C_3 = 1_{180^o}$,$C_4 = 1_{45^o}$, $C_5 = 1_{180^o}$, $C_6 = 1_{45^o}$, $C_7 = 1_{180^o}$
D	$C_1 = 1_{0^o}$, $C_2 = 1_{30^o}$, $C_7 = 1_{60^o}$,$C_8 = 1_{45^o}$,$C_9 = 1_{60^o}$, $C_{10} = 1_{30^o}$, $C_{14} = 1_{0^o}$, $C_{16} = 1_{30^o}$, $C_{17} = 1_{60^o}$, $C_{22} = 1_{45^o}$, $C_{23} = 1_{60^o}$, $C_{24} = 1_{30^o}$, $C_{25} = 1_{0^o}$, $C_{29} = 1_{30^o}$
E	$C_5 = 0.5_{30^o}$, $C_{10} = 1_{60^o}$, $C_{15} = 0.5_{90^o}$, $C_{20} = 1_{120^o}$, $C_{25} = 0.5_{150^o}$, $C_{30} = 1_{180^o}$
F	$C_1 = 0.7_{0^o}$, $C_7 = 0.35_{45^o}$, $C_{13} = 0.7_{90^o}$,$C_{19} = 0.35_{135^o}$,$C_{25} = 0.7_{180^o}$
G	$C_3 = 0.1_{0^o}$, $C_6 = 0.5_{180^o}$, $C_9 = 0.1_{0^o}$, $C_{12} = 0.3_{180^o}$, $C_{15} = 2_{0^o}$, $C_{18} = 0.1_{180^o}$, $C_{21} = 0.5_{0^o}$, $C_{24} = 0.1_{180^o}$, $C_{27} = 0.3_{0^o}$, $C_{30} = 2_{180^o}$

Table 4.1: Excitation vector C_i for different cases studied.

The figures presented on next pages show the power loss distributions obtained with Matlab for different combinations of the antennas complex weights C_i. These results were compared with those obtained directly from CST when using the "*Combined Results*" option, showing identical power loss pattern. Our preliminary results demonstrate different heating patterns synthesis as it will be seen on the following pictures.

It must be mentioned that the advantage of using Matlab instead of CST for the post-processing, resides in the capacity to generate a simple script file to apply a minimax function [35] using the combined field (equation 4.2.1) and a goal heating power distribution.

This way, the weights C_i can be numerically optimized to synthesize a desired heating pattern. **The best-case scenario** would be that one in which the individual antenna fields at the sample $E_{i_{z_{SAMPLE}}}(x, y)$ would form a *complete and orthogonal basis*, so that, any power loss pattern could be created inside the sample. Thus, we are developing such numerical optimization technique to synthesize different objective shapes in the heating pattern.

- **CASE A**

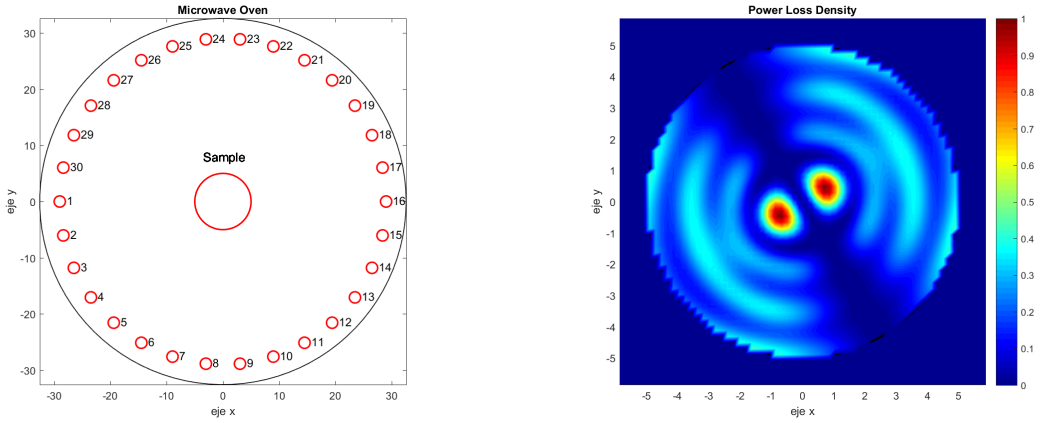

(a) Antennas Case A

(b) P_{LOSS} Case A

Figure 4.8: Normalized Power Loss Density for CASE A.

For instance, when all the antennas are uniformly and in-phase fed (case A in Table 4.1), a heating pattern concentrated in the center of the sample with two lobes is created as shown in Figure 4.8. However, it presents a minimum just in the center of the figure, so it would be interesting to get the center properly heated (as we discuss in other cases).

On the contrary, other phased-array combination as the one of case B in Table 4.1, provide higher heating in the outer region of the sample as shown in Figure 4.9 or 4.10. By phasing the array of antennas, the patterns obtained can be rotated, so that different inner or outer regions of the sample can be heated.

- **CASE B**

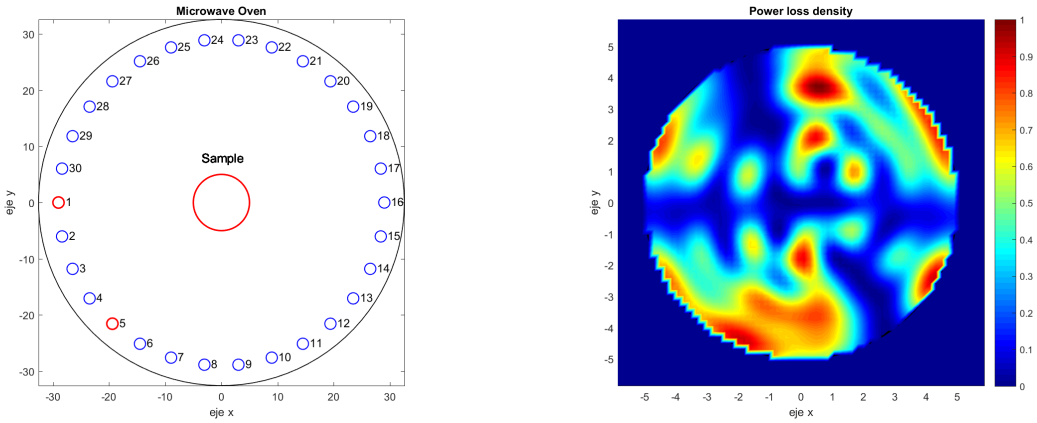

(a) Antennas Case B (b) P_{LOSS} Case B

Figure 4.9: Normalized Power Loss Density for CASE B.

- **CASE C**

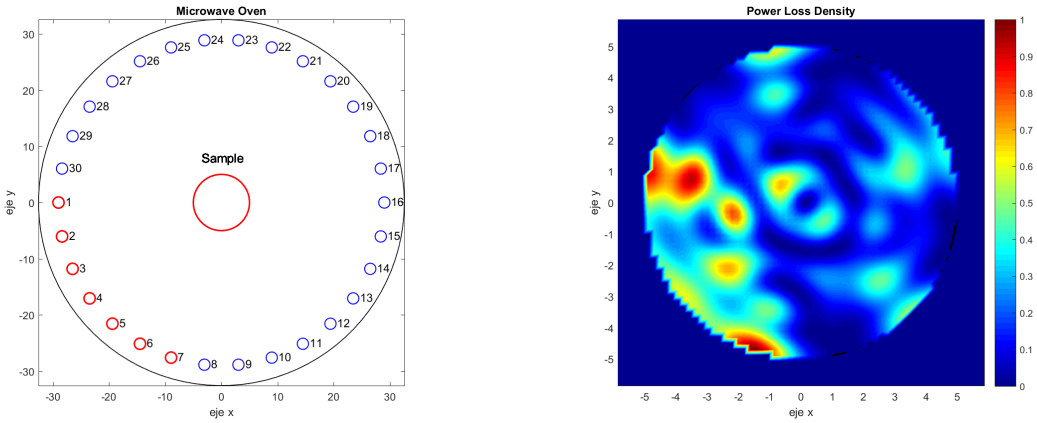

(a) Antennas Case C (b) P_{LOSS} Case C

Figure 4.10: Normalized Power Loss Density for CASE C.

Unlike the heating distribution of case A (Figure 4.8) which showed two lobes when all the antennas were exciting the oven, in this cases different patterns can be seen. In case B (Figure 4.9) only with two antennas involved, the pattern seems so distinct maybe because of the variation of amplitude and phase of the antenna 5 ($C_5 = 0.7_{-45^o}$).

However, in case C (Figure 4.10) as antennas 1 to 7 are activated, the heating distribution seems to be focussed on that part of the sample and a little in its center.

- **CASE D**

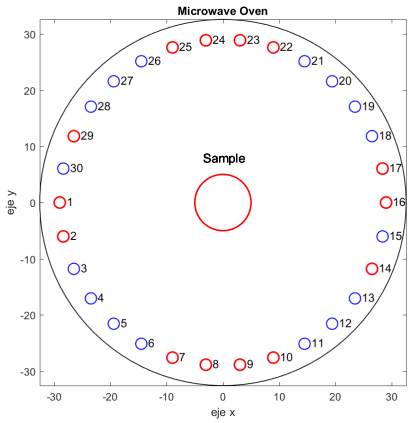

(a) Antennas Case D

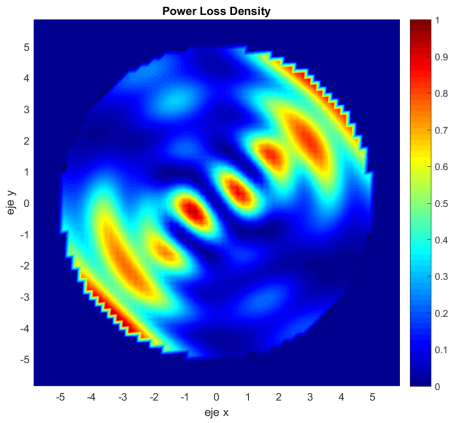

(b) P_{LOSS} Case D

Figure 4.11: Normalized Power Loss Density for CASE D.

- **CASE E**

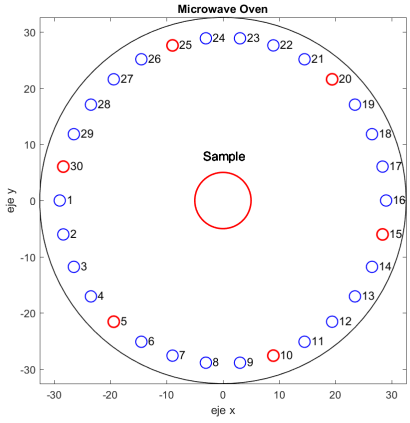

(a) Antennas Case E

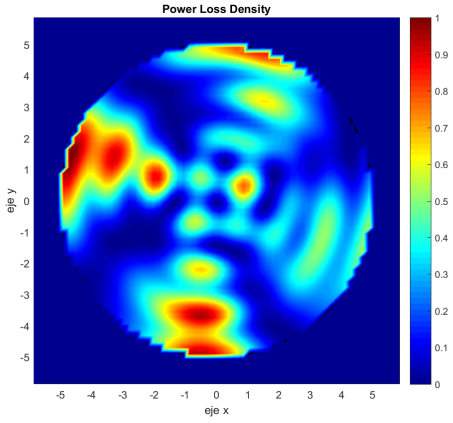

(b) P_{LOSS} Case E

Figure 4.12: Normalized Power Loss Density for CASE E.

This time, when trying to combine patterns of Figure 4.4 and 4.5 in Figure 4.11 (case D), heating focusses on the north-east and south-west region and again presenting two lobes in the center.

In case E (Figure 4.12), it could be considered that the pattern shape is similar to an "*airscrew*" or a "*X*" providing a squared distribution in the middle of the sample with four minimums.

- **CASE F**

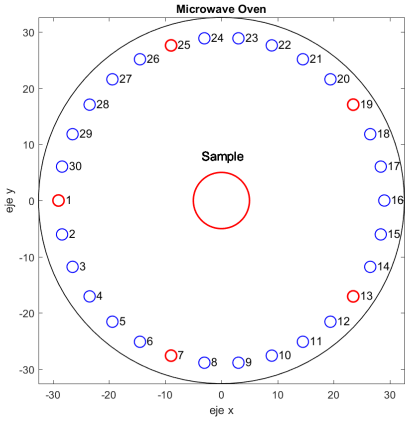

(a) Antennas Case F

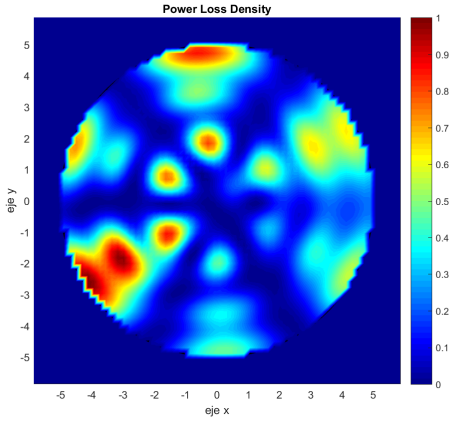

(b) P_{LOSS} Case F

Figure 4.13: Normalized Power Loss Density for CASE F.

- **CASE G**

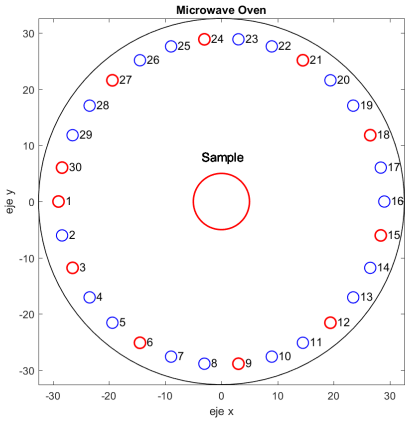

(a) Antennas Case G

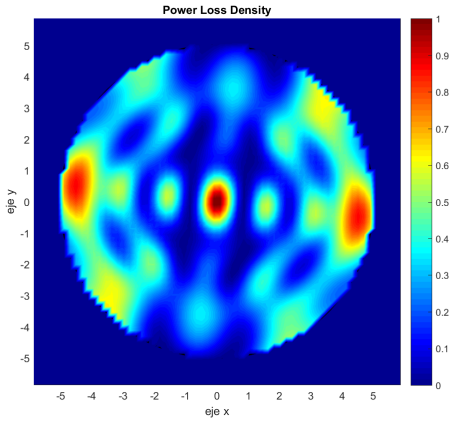

(b) P_{LOSS} Case G

Figure 4.14: Normalized Power Loss Density for CASE G.

Finally, other examples of different heating patterns are case F and G (Figure 4.13 and 4.14). In one hand, the first picture (case F) shows six maximums well distinguished shaped like a "*wheel*", 6 minimums in the azimuthal region and three in the radial one while five antennas feed the oven forming a pentagon.

On the other hand, case G is one of the most interesting distributions due to the fact that the sample's center is properly heated just right in that spot, so changing the exitation weights and testing them following this path, we could finally understand the behavioural pattern of this array of antennas.

4.3 Creating a GUI (Graphical User Interface) with Matlab

In spite of the fact that all of these results discussed in this chapter could have been illustrated by creating functions and programming in Matlab as usual, in order to make easier, faster and more visual all of them, a GUI with Matlab has been created to this aim.

Furthermore, this section has helped to learn more about Matlab and overall to systematize the whole process to finally get the results and to accelerate it.

By using the guide proposed by Matlab, the implementation of this interface has been possible.

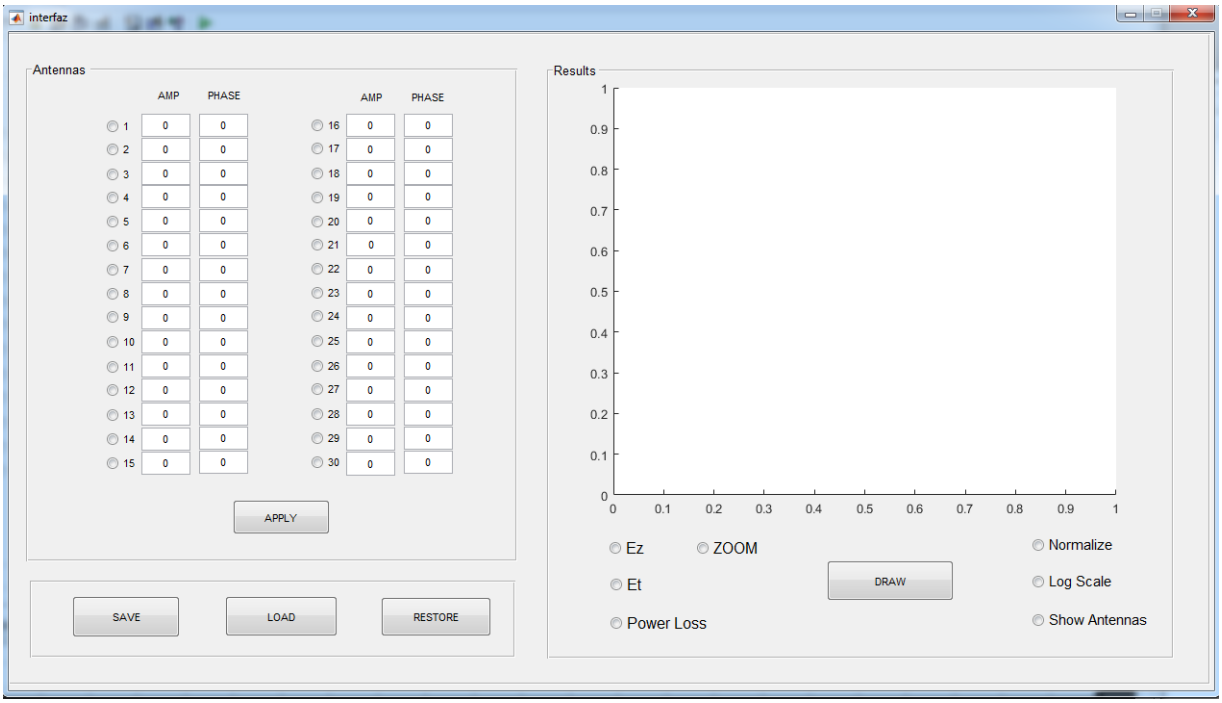

Figure 4.15: GUI of Matlab.

The data exported from CST are loaded from the beginning to be processed in the interface program.

- **Antennas**

  In the interface we can modify the *amplitude* and *phase* of each antenna. We can select one antenna or the combination of antennas we want by pushing the check buttons and editing their amplitude and phase. After the selection, to store the excitation vector (C_i) the *Apply* button has to be pushed.

- **Results**

  It can be chosen what kind of result we want to show. Ez represents the Electric field of the cavity and sample, E_t the transversal component, and *Power Loss* the heating distribution in the whole cavity. *Zoom* is used to see the power loss distribution only in the region of the sample. Button *Draw* is selected when we can see the figure painted.

  Normalize, Log Scale are used to change the scale of the axis, and *Show Antennas* represents the Matlab Structure with the numbered antennas.

- **SAVE, LOAD, RESTORE**

  Button *Save* consist in saving the picture results in a figure.

  Load, as his name says, loads a file (with a predetermined excitation vectors) in the directory we choose to directly show a defined pattern instead of modifying them in the interface.

  Finally, *Restore* button is used to refresh and clear all data and to start again from zero.

As it can be observed, this interface is simple and practical to use and it provides the user saving working time, what happens within long and complicated programs.

Chapter 5

Conclusions and Future Work

Along this project, it has been demonstrated the capability to shape the heating spatial distribution inside the lossy cylindrical sample, using a cylindrical phased-array antenna feeding a cylindrical microwave oven designed and optimized to provide the best results as possible.

By properly selecting the excitation of each individual radiator, changing its amplitude and phase, different heating profiles can be obtained thanks to the generation of dissimilar interference patterns inside the sample and after taking advantage of the symmetry of the cavity and the sample.

It must be noticed that all these results were obtained for coherent radiation using the same frequency (2.45GHz) for all the antennas, so that interference patterns are created inside the sample. This coherent single-frequency interference technique can be combined with multi-tone heating techniques, so that the fields for each frequency are power-additive, and a large variety of heating power distributions can be obtained. Future work will develop that synthesis techniques as the one proposed in [10] using minimax functions [35], in order to systematically optimize the radiators excitation factors C_i (amplitude and phase) which provide a desired heating pattern.

Besides, such a simple, low-cost microwave system would be beneficial to applications where controllable custom-made heating patterns must be created inside the sample to be heated. In this case we have modified the exitation vectors to create different pattern, however, it would be necessary the development of some algorithm that creates and synthesize a desired pattern and give us those weights to manipulate and optimize the good performance of the design to be able to heat a sample the way we want. Hence, that would be innovative for several microwaves applications as hyperthermia in treatment of cancer.

Moreover, continuity restrictions will be forced between adjacent radiators, so that a leaky-wave antenna topology can be used instead of a phased-array antenna. In this way, a single excitation port could create a similar focusing pattern following the methodology developed in [8, 9], avoiding much more complicated power distribution networks associated to phased-arrays [2–4].

We are presenting an idea to develop in the future, which consist in a *cylindrical slotted Leaky-wave antenna* or a *Meandered (Long Slotted) LWA* [36] in order to improve the design proposed in this work and taking into account the advantages of this kind of antennas in contrast with the array exposed.

This cylindrical slotted LWA composed of 30 horizontal slots is fed by a single input port (excited by TE_{10} mode). The amplitude and phase of the 30 radiating slots can be controlled by proper selection of the slots position and size, and the feeding waveguide width instead of the problems that causes selecting every single antenna one by one.

The most important benefit of this initial and preliminary design is that the more complicated distribution network to feed a phased array of 30 individual antennas can be avoided.

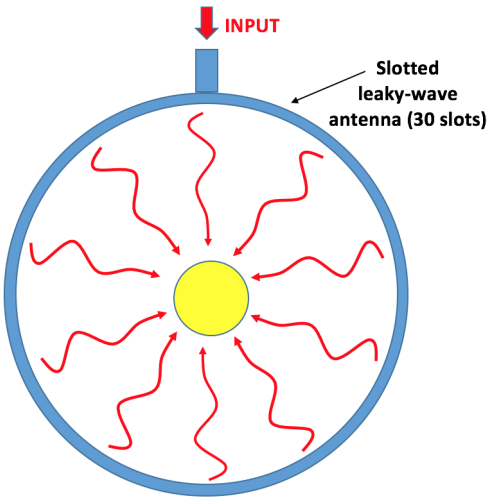

Figure 5.1: Cylindrical Slotted Leaky-wave Antenna.

Bibliography

[1] Adriana Pérez García, José Luis Gómez Tornero, and Juan Monzó. **Microwave Heating Pattern Beamforming Using Cylindrical Phased-Array of Antennas**. *3GMEA. Book of Proceedings*, 2016.

[2] M Bogosanovic and AG Williamson. Antenna array with beam focused in near-field zone. *Electronics letters*, 39(9):1, 2003.

[3] A Buffi, P Nepa, and G Manara. Design criteria for near-field-focused planar arrays. *IEEE Antennas and Propagation Magazine*, 54(1):40–50, 2012.

[4] KD Stephan, JB Mead, DM Pozar, L Wang, and JA Pearce. A near field focused microstrip array for a radiometric temperature sensor. *IEEE transactions on antennas and propagation*, 55(4):1199–1203, 2007.

[5] I Ohtera. Focusing properties of a microwave radiator utilizing a slotted rectangular waveguide. *IEEE transactions on antennas and propagation*, 38(1):121–124, 1990.

[6] G Andrasic, JR James, and JW Hand. Investigation of quasi-leaky-wave applicator using fd-td computations. In *Antennas and Propagation, 1991. ICAP 91., Seventh International Conference on (IEE)*, pages 584–587. IET, 1991.

[7] Alejandro Javier Martínez-Ros, José Luis Gómez-Tornero, Francisco Javier Clemente-Fernández, and Juan Monzó-Cabrera. Microwave near-field focusing properties of width-tapered microstrip leaky-wave antenna. *IEEE Transactions on Antennas and Propagation*, 61(6):2981–2990, 2013.

[8] Jose-Luis Gomez-Tornero. Unusual tapering of leaky-wave radiators and their applications. In *Proceedings of the 5th European Conference on Antennas and Propagation (EUCAP)*, pages 821–824. IEEE, 2011.

[9] Jose Luis Gomez-Tornero. Analysis and design of conformal tapered leaky-wave antennas. *IEEE Antennas and Wireless Propagation Letters*, 10:1068–1071, 2011.

[10] José Luis Gómez-Tornero, Alejandro Javier Martínez-Ros, and Juan Monzó-Cabrera. Demonstration of simple electronic near-field beamforming using multitone microwave signals with a leaky-wave focused applicator. *IEEE Antennas and Wireless Propagation Letters*, 14:143–146, 2015.

[11] CST Computer Simulation Technology. `www.cst.com`.

[12] C-K Chou. Application of electromagnetic energy in cancer treatment. *IEEE transactions on instrumentation and measurement*, 37(4):547–551, 1988.

[13] F Kristian Storm. *Hyperthermia in cancer therapy.* GK Hall, 1983.

[14] Jill van der Zee. Heating the patient: a promising approach? *Annals of oncology*, 13(8):1173–1184, 2002.

[15] Leonard L Gunderson, Joel E Tepper, and Jeffrey A Bogart. *Clinical radiation oncology.* Elsevier Health Sciences, 2015.

[16] P Wust, B Hildebrandt, G Sreenivasa, B Rau, J Gellermann, H Riess, R Felix, and PM Schlag. Hyperthermia in combined treatment of cancer. *The lancet oncology*, 3(8):487–497, 2002.

[17] Paul F Turner. Regional hyperthermia with an annular phased array. *IEEE Transactions on Biomedical Engineering*, (1):106–114, 1984.

[18] AW Guy, Chung-Kwang Chou, and KH Luk. 915-mhz phased-array system for treating tumors in cylindrical structures. *IEEE transactions on microwave theory and techniques*, 34(5):502–507, 1986.

[19] FA Gibbs Jr. Clinical evaluation of a microwave/radiofrequency system (bsd corporation) for induction of local and regional hyperthermia. *The Journal of microwave power*, 16(2):185–192, 1981.

[20] Frederic A Gibbs, Michael D Sapozink, Kathy S Gates, and J Robert Stewart. Regional hyperthermia with an annular phased array in the experimental treatment of cancer: Report of work in progress with a technical emphasis. *IEEE transactions on biomedical engineering*, (1):115–119, 1984.

[21] Jonathan E Rhoads. Cancer—principles & practice of oncology. *Annals of Surgery*, 197(1):116, 1983.

[22] MH Rahmani and A Pirhadi. Optimum design of conformal array antenna with a shaped radiation pattern and wideband feeding network. *Applied Computational Electromagnetics Society Journal*, 29(1), 2014.

[23] Lars Josefsson and Patrik Persson. *Conformal array antenna theory and design*, volume 29. John wiley & sons, 2006.

[24] Jaco Du Preez and Saurabh Sinha. *Millimeter-Wave Antennas: Configurations and Applications.* Springer, 2016.

[25] David R Jackson and Arthur A Oliner. Leaky-wave antennas. *Modern Antenna Handbook*, pages 325–367, 2008.

[26] M Ettore. *Analysis and design of efficient planar leaky-wave antennas.* Siena: Universita Degli Studi di Siena, 2008.

[27] Arthur A Oliner and David R Jackson. Leaky-wave antennas. *Antenna Engineering Handbook*, 4:12, 1993.

[28] Isao Ohtera. Diverging/focusing of electromagnetic waves by utilizing the curved leakywave structure: application to broad-beam antenna for radiating within specified wide-angle. *IEEE Transactions on Antennas and Propagation*, 47(9):1470–1475, 1999.

[29] Joshua Radcliffe, Gary Thiele, Robert Penno, Steve Schneider, and Leo Kempel. Microstrip leaky wave antenna performance on a curved surface. In *2006 IEEE Antennas and Propagation Society International Symposium*, pages 4247–4250. IEEE, 2006.

[30] Onofrio Losito. Design of conformal tapered leaky wave antenna. *PIER Online*, 3(8):1316–1320, 2007.

[31] CM Rappaport and FR Morgenthaler. Localized hyperthermia with electromagnetic arrays and the leaky-wave troughguide applicator. *IEEE transactions on microwave theory and techniques*, 34(5):636–643, 1986.

[32] Antoni J Canos, José M Catala-Civera, Felipe L Penaranda-Foix, Juan Monzo-Cabrera, and E De los Reyes. A new empirical method for extracting unloaded resonant frequencies from microwave resonant cavities. In *Microwave Symposium Digest, 2003 IEEE MTT-S International*, volume 3, pages 1823–1825. IEEE, 2003.

[33] Alejandro Díaz Morcillo and Juan Monzó Cabrera. *Líneas de transmisión, guías de onda y cavidades resonantes*. Universidad Politécnica de Cartagena, 2007.

[34] AC Metaxas, , and Roger J Meredith. *Industrial microwave heating*. Number 4. IET, 1983.

[35] E Polak, JO Royset, and RS Womersley. Algorithms with adaptive smoothing for finite minimax problems. *Journal of Optimization Theory and Applications*, 119(3):459–484, 2003.

[36] Frank L Whetten and Constantine A Balanis. Meandering long slot leaky-wave waveguide-antennas. *IEEE Transactions on antennas and propagation*, 39(11):1553–1560, 1991.

[37] The MathWorks, Natick, MA, USA. Solve minimax constraint problem–matlab: fminimax `http://www.mathworks.es/es/help/optim/ug/fminimax.html`, 2016.

[38] W Gee, S Lee, R Mitra, C Cain, and R Magin. Focused array hyperthermia applicator: Theory and experiment. In *Antennas and Propagation Society International Symposium, 1983*, volume 21, pages 261–264. IEEE, 1983.

[39] PN Fletcher and M Dean. Derivation of orthogonal beams and their application to beamforming in small phased arrays. *IEE Proceedings-Microwaves, Antennas and Propagation*, 143(4):304–308, 1996.